nature plants

ARTICLES

https://doi.org/10.1038/s41477-022-01151-9

Check for updates

Boosting plant genome editing with a versatile CRISPR-Combo system

Changtian Pan[1], Gen Li[1], Aimee A. Malzahn[1], Yanhao Cheng[1], Benjamin Leyson[1], Simon Sretenovic[1], Filiz Gurel[1], Gary D. Coleman[1,2] and Yiping Qi[1,2] ✉

CRISPR-Cas9, its derived base editors and CRISPR activation systems have greatly aided genome engineering in plants. However, these systems are mostly used separately, leaving their combinational potential largely untapped. Here we develop a versatile CRISPR-Combo platform, based on a single Cas9 protein, for simultaneous genome editing (targeted mutagenesis or base editing) and gene activation in plants. We showcase the powerful applications of CRISPR-Combo for boosting plant genome editing. First, CRISPR-Combo is used to shorten the plant life cycle and reduce the efforts in screening transgene-free genome-edited plants by activation of a florigen gene in *Arabidopsis*. Next, we demonstrate accelerated regeneration and propagation of genome-edited plants by activation of morphogenic genes in poplar. Furthermore, we apply CRISPR-Combo to achieve rice regeneration without exogenous plant hormones, which is established as a new method to predominately enrich heritable targeted mutations. In conclusion, CRISPR-Combo is a versatile genome engineering tool with promising applications in crop breeding.

Since its first demonstration as an RNA-guided nuclease[1], CRISPR-Cas9 has been rapidly applied for genome editing in eukaryotes, including plants[2,3]. It has been predominantly used for targeted mutagenesis through error-prone, non-homologous end-joining (NHEJ) repair. In recent years, Cas9 nickase (Cas9n)-derived base editors such as cytosine base editors (CBEs) and adenine base editors (ABEs) have gained momentum for inducing precise base changes in genomes[4,5]. Dual base editors that confer simultaneous C-to-T and A-to-G base edits have also been developed and include the synchronous programmable adenine and cytosine editors SPACE[6], A&C-BEmax[7] and Target-ACEmax[8], which have been demonstrated in human cells, and saturated targeted endogenous mutagenesis editors (STEMEs), which have been demonstrated in plants[9]. In addition, a platform was developed for simultaneous adenine base editing, cytosine base editing and NHEJ mutagenesis in plant genomes[10]. However, these multifunctional CRISPR systems are limited in their capabilities since they only facilitate genome editing.

Aside from genome editing, CRISPR-Cas9 has been repurposed for genome reprogramming at the transcriptional level. CRISPR activation (CRISPRa) systems allow for transcriptional activation and were developed in both mammalian[11,12] and plant cells[13–15]. These CRISPRa systems are based on a nuclease-deactivated Cas9 (dCas9) that retains single guide RNA (sgRNA)-mediated DNA-binding activity[1]. To achieve simultaneous genome editing and transcriptional regulation, multiple constructs expressing orthogonal Cas9 proteins were codelivered into mammalian cells[16,17]. However, this approach is less applicable in plants because of the low efficiency of *Agrobacterium*-mediated cotransformation of multiple Cas9 constructs[18,19]. Previous studies have shown that the DNA cleavage activity of Cas9 and Cas12a can be abolished without compromising DNA binding by using truncated protospacers[20,21]. On the basis of this principle, nuclease active Cas9-VPR and AsCas12a-VPR fusions were engineered for orthogonal gene knockout and transcriptional activation in mammalian cells[20,22]. However, a robust CRISPR system for simultaneous base editing and transcriptional activation is yet to be developed in any organism.

Recently, we developed a highly potent CRISPR-Act3.0 system for gene activation in plants which uses an engineered sgRNA2.0 scaffold for recruiting transcriptional activators[23]. We postulated that CRISPR-Act3.0 could be used to further develop a sophisticated CRISPR platform for simultaneous genome editing and gene activation since the transcriptional activator is recruited by the sgRNA scaffold, not by Cas protein fusions as used in earlier studies[20,22]. Tasking two distinct functionalities to Cas9 and sgRNA, respectively, would enable the development of truly orthogonal genome editing and gene activation systems. On the basis of this design principle, we developed a versatile CRISPR-Combination (CRISPR-Combo) platform for robust orthogonal genome editing (targeted mutagenesis or base editing) and gene activation in plants. We showed the orthogonal CRISPR-Combo functionalities in rice and tomato protoplasts. To demonstrate CRISPR-Combo as a powerful technology, we applied it in *Arabidopsis*, poplar and rice to promote flowering and accelerate plant regeneration and propagation while simultaneously enriching for high-efficiency genome-edited plants.

Results

CRISPR-Combo for targeted mutagenesis and gene activation. To assess inactivation of the DNA cleavage activity of CRISPR-Cas9 through sgRNA engineering, we tested targeted mutagenesis by Cas9 at *OsYSA* and *OsMAPK5* loci using different protospacer lengths in rice protoplasts. Restriction fragment length polymorphism (RFLP) analysis showed that 17- to 20-nucleotide (nt) protospacers conferred efficient mutagenesis while 14- to 16-nt protospacers were unable to cause mutations at both target sites (Extended Data Fig. 1a). On the basis of our previous developed CRISPR activation system CRISPR-dCas9-Act3.0 (ref. [23]), we created the CRISPR-Cas9-Act3.0 (Cas9-Act3.0) system by replacing the deactivated Cas9 (dCas9) with wild-type Cas9 (Extended Data Fig. 1b) and comparison between Cas9-Act3.0 and Cas9 coupled

[1]Department of Plant Science and Landscape Architecture, University of Maryland, College Park, MD, USA. [2]Institute for Bioscience and Biotechnology Research, University of Maryland, Rockville, MD, USA. ✉e-mail: yiping@umd.edu

with a normal sgRNA (gR1.0) scaffold showed that they had comparable editing activities at two independent target sites when coupled with sgRNAs of 20-nt protospacers (Extended Data Fig. 1b). Reduction of the protospacers to 15-nt abolished editing activity of both systems (Extended Data Fig. 1b). These data indicate that Cas9-Act3.0 possesses wild-type levels of Cas9 nuclease activity, which can be deactivated with short protospacers. Next, we assessed gene activation by Cas9-Act3.0 with the sgRNA2.0 scaffold[14] and variable protospacer lengths. Robust transcriptional activation of the target genes (*OsGW7* and *OsER1*) was observed with short 14- to 16-nt protospacers (Extended Data Fig. 1c). By contrast, longer protospacers (for example, 17- to 20-nt) showed reduced gene activation efficiency (Extended Data Fig. 1c), suggesting targeted mutagenesis had occurred at these sites which prevented the further binding of the activation system to the promoters.

These experiments demonstrated the first CRISPR-Combo system that could allow for simultaneous targeted mutagenesis and gene activation in plants in an orthogonal manner programmed by co-expression of gR1.0 and sgRNA2.0 (gR2.0) scaffolds with 20-nt protospacers and 15-nt protospacers, respectively (Fig. 1a). To benchmark this CRISPR-Combo system, we further tested whether Cas9-Act3.0 enables orthogonal gene activation *OsBBM1* and mutagenesis of *OsGW2* and *OsGN1a* with both NGG and NGC protospacer adjacent motifs (PAMs) (Fig. 1b,c and Supplementary Table 1). At the canonical NGG PAM site, Cas9-Act3.0 in the CRISPR-Combo system showed a comparable *OsBBM1* activation level to that of dCas9-Act3.0 (Fig. 1c). Not surprisingly, both systems failed to activate *OsBBM1* at an NGC non-canonical PAM site (Fig. 1c). We next compared Cas9-Act3.0 with Cas9 at editing two NGG PAM sites and two NGC PAM sites. Both systems showed higher editing efficiency at the preferred NGG PAM sites (Fig. 1c). Importantly, there was no significant difference between Cas9-Act3.0 and Cas9 on genome editing activity (Fig. 1c). We further assessed the system in tomato by simultaneous activation of *SFT* and targeted mutagenesis of *SolyA7* (Supplementary Table 1). Cas9-Act3.0 even induced a significantly higher activation of *SFT* compared with dCas9-Act3.0 (Fig. 1d). The editing efficiency of Cas9-Act3.0 at the *SolyA7* target site was substantially reduced compared with Cas9 but remained high. Furthermore, Cas9-Act3.0 resulted in similar NHEJ mutation profiles to those of Cas9 at the target sites in rice and tomato protoplasts, both for deletion positions and deletion sizes (Extended Data Fig. 2a,b). Next-generation sequencing (NGS) showed that Cas9-Act3.0 with 15-nt protospacer, unlike the 20-nt protospacer control, did not result in detectable genome editing events in the promoter regions of *OsBBM1* and *SFT*, based on the protoplast assay of rice and tomato, respectively (Extended Data Fig. 2c and Supplementary Table 1). This confirms the orthogonal functions of the CRISPR-Combo system.

Recently, the Cas9 variant SpRY was demonstrated for PAM-less genome editing in human cells[24] and plants[25–27]. On the basis of the CRISPR-Combo principle, we further demonstrated that SpRY-Act3.0 enables orthogonal gene activation and mutagenesis by simultaneously targeting *OsBBM1*, *OsGW2* and *OsGN1a* at both NGG and NGC PAMs (Extended Data Fig. 3a and Supplementary Table 1). At both the NGG and NGC PAM sites, SpRY-Act3.0 systems induced comparable activation efficiencies ~10- to 30-fold gene activation compared to the dSpRY-Act3.0 system (Extended Data Fig. 3a). We further compared SpRY-Act3.0 and SpRY for genome editing at *OsGW2* and *OsGN1a*. SpRY-Act3.0 retained genome editing capability, albeit with lower editing efficiency at three out of four target sites (Extended Data Fig. 3b). Furthermore, SpRY-Act3.0 and SpRY showed similar NHEJ mutation profiles (Extended Data Fig. 3c,d). These results suggest that SpRY-Act3.0 allows for simultaneous PAM-less targeted mutagenesis and gene activation.

CRISPR-Combo for base editing and gene activation. We next sought to develop CRISPR-Combo systems suitable for simultaneous base editing and gene activation. For C-to-T base editing, CBE-Cas9n-Act3.0 was generated by implanting the highly efficient A3A/Y130F-Cas9-UGI[28–30] into the CRISPR-Act3.0 system[23] (Fig. 2a,b). For A-to-G base editing, ABE8e-Cas9n[25,31] was used to generate ABE-Cas9n-Act3.0 (Fig. 2a,b). These BE-Cas9n-Act3.0 systems were first assessed in rice protoplasts by simultaneous activation of *OsBBM1* and mutagenesis of *OsALS* and *OsEPSPS* (Supplementary Table 1). These systems were capable of simultaneous base editing and gene activation, resulting in similar gene activation levels to those that contained activation sgRNAs alone, although ABE-Cas9n-Act3.0 drastically reduced the activation potency (Fig. 2c), which might be partly attributed to ABE8e dimerization[32]. However, the CBE-Cas9n-Act3.0 and ABE-Cas9n-Act3.0 systems had similar base editing activity to the canonical CBE-Cas9n and ABE-Cas9n systems (Fig. 2c). We further tested CBE-Cas9n-Act3.0 in tomato protoplasts. The results showed high gene activation potency when both activation and base editing sgRNAs were co-expressed (Fig. 2d) and there was slight reduction of base editing efficiency when compared to CBE-Cas9n (Fig. 2d). Compared to the canonical base editors, the base editing windows were not altered for either CBE-Cas9n-Act3.0 or ABE-Cas9n-Act3.0 (Extended Data Fig. 4a-c). To further evaluate the editing activity of CBE-Cas9n-Act3.0 and ABE-Cas9n-Act3.0 systems with 15-nt protospacer, the editing events were analysed at promoter region of both *OsBBM1* and *SFT* using NGS. The CBE-Cas9n-Act3.0 and ABE-Cas9n-Act3.0 systems expressing empty sgRNA and 20-nt protospacer were used for negative and positive controls, respectively (Extended Data Fig. 4d and Supplementary Table 1). In both rice and tomato protoplasts, CBE-Cas9n-Act3.0 and ABE-Cas9n-Act3.0 systems induced efficient C-to-T or A-to-G conversion with a 20-nt protospacer but undetectable base editing frequency using a 15-nt protospacer or an empty sgRNA (Extended Data Fig. 4d).

To broaden the targeting scope, we again harnessed SpRY and generated CBE-SpRYn-Act3.0 and ABE-SpRYn-Act3.0. By simultaneously targeting *OsBBM1*, *OsALS* and *OsEPSPS*, we found that CBE-SpRYn-Act3.0 only generated a low level of gene activation of *OsBBM1* in rice protoplasts, while ABE-SpRYn-Act3.0 failed to activate this gene (Extended Data Fig. 5a), consistent with previous observation of low activation potency of dSpRY-Act3.0 (ref. [23]) and ABE-Cas9n-Act3.0 (Fig. 2c). However, both CBE-SpRYn-Act3.0 and ABE-SpRYn-Act3.0 systems yielded relatively comparable base editing efficiency (Extended Data Fig. 5b) and base editing windows to the canonical CBE and ABE controls (Extended Data Fig. 5c,d).

Accelerated breeding of transgene-free genome-edited plants. To demonstrate powerful applications of CRISPR-Combo, we focused on addressing some of the most pressing challenges in plant genome editing. The first challenge is achieving accelerated breeding of genome-edited transgene-free plants. We recently showed that activation of the florigen gene *AtFT* in *Arabidopsis* by CRISPR-Act3.0 promoted early flowering[23]. We reasoned that a CRISPR-Combo-based genome editing pipeline with simultaneous activation of *AtFT* would have three benefits compared to the traditional genome editing experiments. First, it would drastically reduce the time to flowering. Second, the transgenic plants with early flowering phenotypes would suggest high levels of CRISPR-Combo expression, aiding the identification of high-frequency genome-edited lines. Third, selection of standard flowering plants in the next generation would drastically reduce the screening efforts for transgene-free genome-edited plants by at least 75%, based on the Mendelian segregation ratios of a single transgene.

To develop this improved genome editing pipeline, we decided to test two CRISPR-Combo systems, Cas9-Act3.0 for targeted

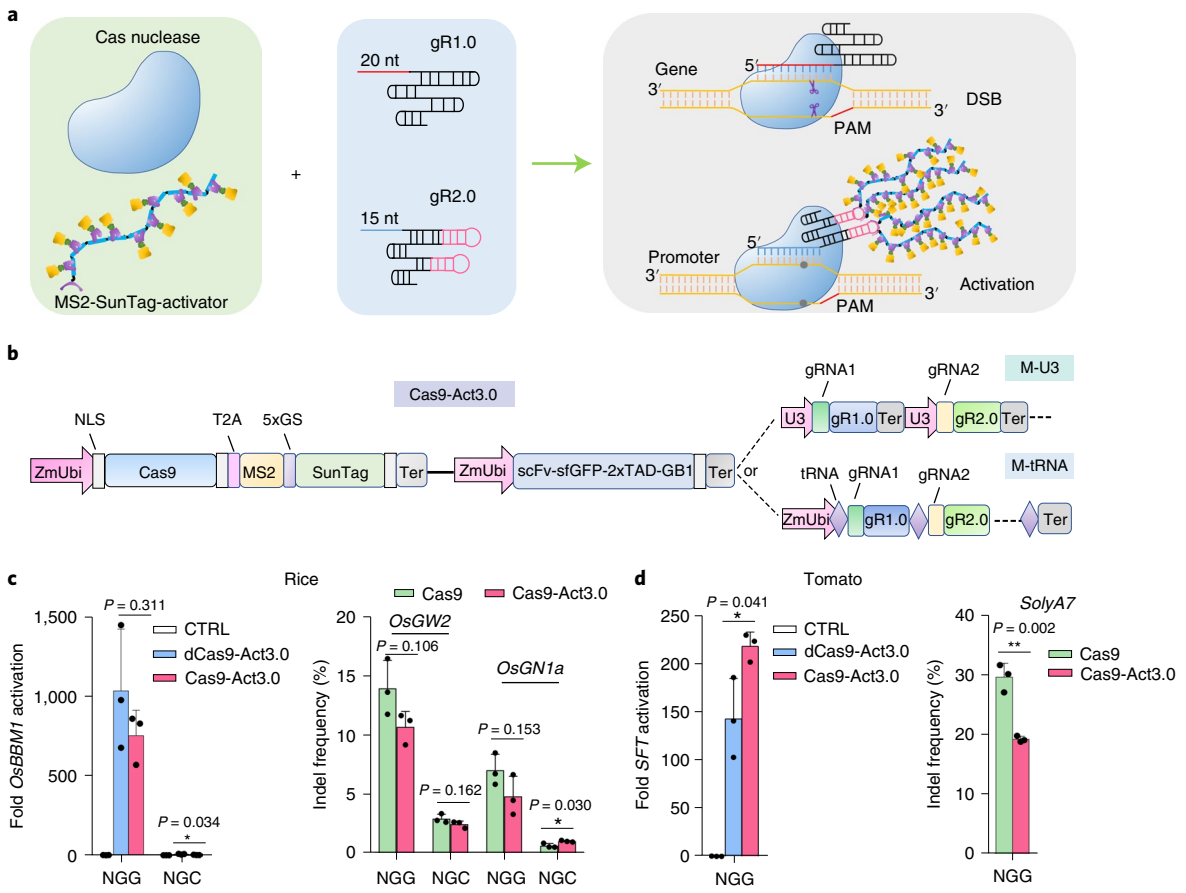

Fig. 1 | Development of the Cas9-Act3.0 system for simultaneous targeted mutagenesis and gene activation. a, Diagram of the Cas9-Act3.0-induced simultaneous targeted mutagenesis and activation. The Cas9-Act3.0 system consists of a catalytically active Cas9 nuclease and MS2 bacteriophage coat protein (MCP)-SunTag-activator complex and two kinds of single guide (sgRNA) scaffolds gR1.0 and gR2.0. Each SunTag peptide can recruit ten copies of activator 2xTAL activation domain (TAD) by single-chain variable fragment (scFV) of GCN4 antibody fused to a super-folder GFP (sfGFP). gR2.0 contains two MS2 RNA aptamers (in red) which can bind the MCP-SunTag-2xTAD transcriptional activation complex to activate gene expression with a 15-nt protospacer and Cas9 nuclease without inducing double-strand breaks (DSB). Simultaneously, gR1.0 induces DSB with a 20-nt protospacer and Cas9 nuclease. **b**, Schematic illustration of Cas9-Act3.0 expression vectors. GS, glycine–serine linker; SunTag, ten tandem repeats of GCN4 peptide; Ter, terminator; M-U3, multiple tandem repeats of independent U3 promoter-based gR1.0 and gR2.0 expression cassettes; M-tRNA, multiple transfer RNA-mediated gR1.0 and gR2.0 expression cassettes driven by a Pol II promoter ZmUbi; NLS, nuclear localization signal. **c**,**d**, Cas9-Act3.0 induces simultaneous gene activation and indel mutation in rice (**c**) and tomato (**d**) protoplasts, respectively. One 15-nt protospacer each for *OsBBM1* and *SFT* was separately cloned into the gR2.0 scaffold for Cas9-Act3.0-mediated gene activation. One 20-nt protospacer each for *OsGW2*, *OsGN1a* and *SolyA7* was separately cloned into the gR1.0 scaffold for Cas9-Act3.0-mediated genome editing. The dCas9-Act3.0 activation system and Cas9 genome editing system are used as controls. M-tRNA and M-U3 systems were used for rice and tomato assays, respectively. For the quantitative reverse-transcription PCR (qRT–PCR) assays, T-DNA vectors without sgRNAs served as the negative control (CTRL). *OsTubulin* and *SlUbi3* are selected as the endogenous control genes for rice and tomato, respectively. Each dot represents an individual biological replicate. Error bar, mean ± s.d. ($n = 3$ independent experiments). *P* values were obtained using the two-tailed Student's *t*-test. $^{*}P < 0.05$, $^{**}P < 0.01$.

mutagenesis and CBE-Cas9n-Act3.0 for C-to-T base editing, in *Arabidopsis*. A strong constitutive promoter AtUBQ10 was used to express both Cas9 and Cas9n. For Cas9-Act3.0, multiplexed genome editing (GE) of *AtPYL1* and *AtAP1* was pursued with simultaneous activation of *AtFT* (Fig. 3a and Supplementary Table 1). Extra-early flowering T_1 plants were observed for this construct but not for the Cas9 genome editing control construct or the Cas9-Act3.0 control without the *AtFT* activation sgRNA (Fig. 3a). Similarly, a multiplexed CBE-Cas9n-Act3.0 construct was made for simultaneous base editing of two herbicide target genes (*AtALS* and *AtACC2*) with concurrent activation of *AtFT* (Supplementary Table 1). This construct, not the CBE-nCas9 base editor control, also resulted in T_1 transformants with extra-early flowering phenotypes (Fig. 3a). We quantified gene editing frequencies for T_1 lines by NGS of PCR amplicons. For Cas9 and Cas9-Act3.0-GE (without *AtFT* activation) constructs, both systems produced comparable editing frequencies at the *AtPYL1* and *AtAP1* sites (Fig. 3b). For the Cas9-Act3.0-A + GE construct for simultaneous gene activation and editing, T_1 plants were classified into three groups: extra-early flowering, early flowering and standard (for example, wild-type-like flowering time). Extra-early flowering plants showed overall higher genome editing frequencies, especially compared to the standard flowering plants ($P = 0.021$ at *AtPYL1* and $P = 0.088$ at *AtAP1*) (Fig. 3b). Compared to the standard plants resulting from the Cas9 and Cas9-Act3.0-GE constructs, the median editing frequencies were elevated for Cas9-Act3.0-A + GE extra-early flowering plants (Fig. 3b). We next quantified C-to-T base editing frequencies for the T_1 plants from the multiplexed CBE-Cas9n-Act3.0 construct. The extra-early flowering plants showed significantly higher base-editing frequencies than the early flowering ($P = 0.018$ and $P = 0.003$) and standard

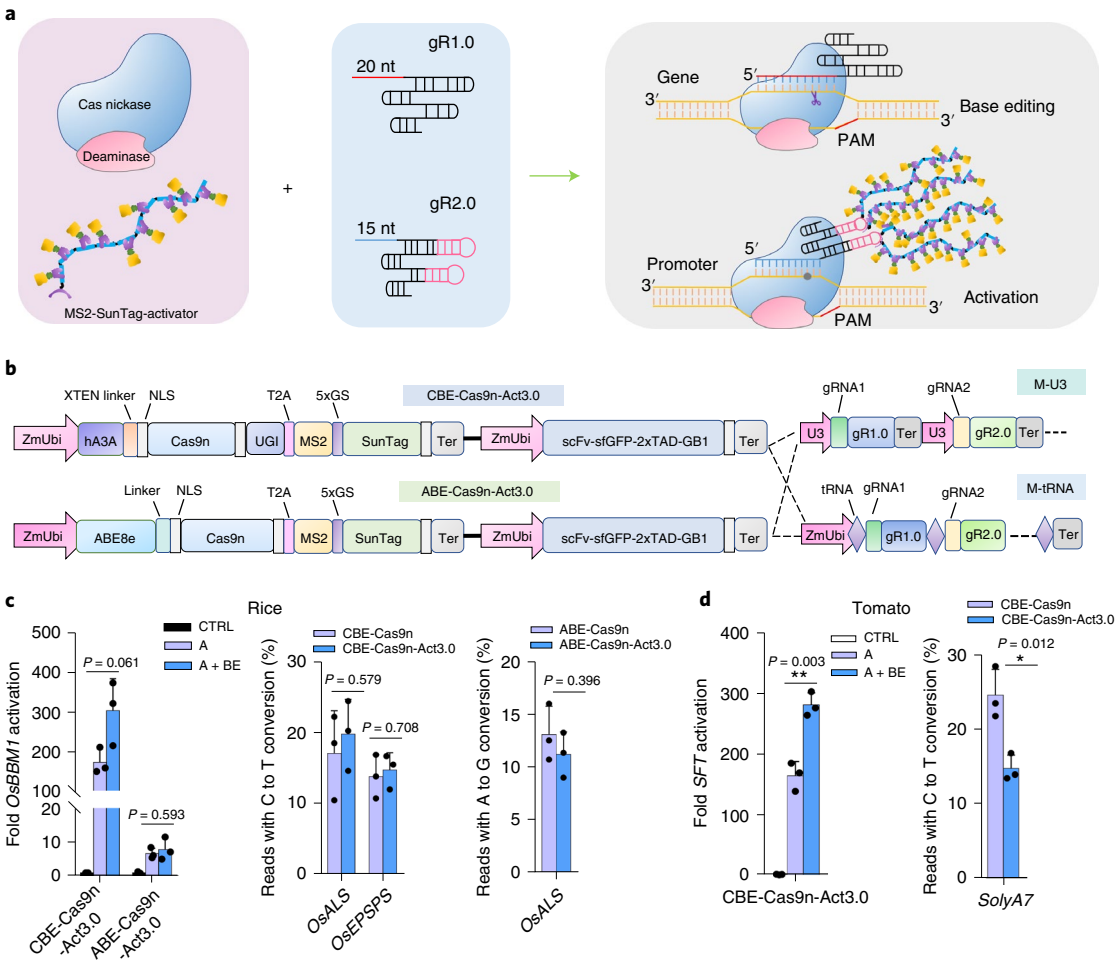

Fig. 2 | Development of the CBE-Cas9n-Act3.0 and ABE-Cas9n-Act3.0 systems for simultaneous base editing and gene activation. a, Diagram of the cytosine base editor (CBE)-Cas9n-Act3.0- and adenine base editor (ABE)-Cas9n-Act3.0-induced simultaneous base editing and gene activation. CBE-Cas9n-Act3.0 and ABE-Cas9n-Act3.0 systems consist of a Cas9 nickase fused with a cytidine or adenine deaminase, an MCP-SunTag-activator complex and gR1.0 and gR2.0. Each SunTag peptide can recruit ten copies of activator 2xTAD by scFV fused to sfGFP (scFV-sfGFP). The gR2.0 contains two MS2 RNA aptamers (in red) which can bind the MCP-SunTag-2xTAD transcriptional activation complex and activate gene expression with a 15-nt protospacer and CBE/ABE-Cas9n. Simultaneously, gR1.0 induces base editing with a 20-nt protospacer and CBE/ABE-Cas9n. **b**, Schematic illustration of CBE-Cas9n-Act3.0 and ABE-Cas9n-Act3.0 expression vectors. GS, glycine–serine linker; NLS, nuclear localization signal; SunTag, ten tandem repeats of GCN4 peptide; Ter, terminator; hA3A/Y130F, human APOBEC3A; UGI, uracil DNA glycosylase inhibitor; ABE8e, adenine deaminase; M-U3, multiple tandem repeats of independent U3 promoter-based gR1.0 and gR2.0 expression cassettes; M-tRNA, multiple tRNA-mediated gR1.0 and gR2.0 expression cassettes driven by a Pol II promoter ZmUbi; XTEN linker, a 16 amino acid (aa) flexible linker. **c**,**d**, CBE-Cas9n-Act3.0 and ABE-Cas9n-Act3.0 induce simultaneous gene activation and base editing in rice (**c**) and tomato (**d**) protoplasts. One 15-nt protospacer of *OsBBM1* and *SFT* was cloned into each gR2.0 scaffold for CBE- and ABE-Cas9n-Act3.0-mediated gene activation, respectively. One 20-nt protospacer for *OsALS, OsEPSPS* and *SolyA7* was cloned into each gR1.0 scaffold for CBE- and ABE-Cas9n-Act3.0-mediated base editing, respectively. A, CBE/ABE-Cas9n-Act3.0 mediates target gene activation with the gR2.0 scaffold; A + BE, CBE/ABE-Cas9n-Act3.0 mediates simultaneous gene activation and base editing with both gR1.0 and gR2.0 scaffolds. Base editing constructs CBE-Cas9n and ABE-Cas9n were used as controls. M-tRNA and M-U3 systems were used for rice and tomato assays, respectively. For the quantitative reverse-transcription PCR (qRT-PCR) assays, T-DNA vectors without sgRNAs served as the negative CTRL. *OsTubulin* and *SlUbi3* are selected as the endogenous control genes for rice and tomato, respectively. Each dot represents an individual biological replicate. Error bar, mean ± s.d. ($n = 3$ independent experiments). *P* values were obtained using the two-tailed Student's *t*-test. $^{*}P < 0.05$, $^{**}P < 0.01$.

plants ($P = 0.0004$ and $P = 0.0002$) at the *AtALS* site and the *AtACC2* site, respectively (Fig. 3c). Compared to the conventional CBE-Cas9n vector, the dynamic ranges of base-editing frequencies were much narrower for the extra-early flowering plants of the CBE-Cas9n-Act3.0-A + BE construct at both target sites (Fig. 3c), suggesting extra-early flowering plants had more robust editing across the population.

We next sought to evaluate whether the early flowering phenotype could be reliably used as a phenotypic marker for transgenic plants in the next (T_2) generation. We focused on the progeny of a total of 12 independent extra-early flowering T_1 lines. Plants from each T_2 population were also classified as extra-early flowering, early flowering and standard (Fig. 3d). For the Cas9-Act3.0-A + GE construct, six T_2 populations were examined, with numbers of plants ranging from 94 to 137 per population. The ratios of all extra-early and early flowering plants to the standard plants averaged 2.8 to 1 (Fig. 3e), indicating that nearly all the parental T_1 lines carried only one transfer DNA (T-DNA) integration event. Remarkably, PCR-based genotyping confirmed that standard plants are indeed mostly transgene-free plants with an average of 92% accuracy

(Fig. 3e). Similar results were found for the T_2 plants from the CBE-Cas9n-Act3.0-A + BE (based editing) T_1 lines, where standard plants were confirmed by molecular genotyping as transgene-free plants with an average of 93% accuracy (Fig. 3f). To identify genome-edited lines in these transgene-free plants, we genotyped these T_2 lines by NGS. For the Cas9-Act3.0-A + GE construct, all five T_2 populations generated detectable mutants with line no. 2 having the highest number of genome-edited lines with a median editing frequency of ~50% at the *AtPYL1* site (Supplementary Fig. 1a). Transgene-free homozygous, biallelic and heterozygous *atpyl1* were readily identified in these populations (Supplementary Fig. 1b). The *AtAP1* site was barely mutated, which is probably due to the non-heritable somatic mutations induced in the T_1 plants (Supplementary Fig. 1a). For the CBE-Cas9n-Act3.0-A + BE construct, all five T_2 populations generated base-edited lines (Extended Data Fig. 6a). The editing frequency at the *AtACC2* site was higher than that of the *AtALS* site in each T_2 population (Extended Data Fig. 6a), which is consistent with the data in T_1 lines (Fig. 3c). Nevertheless, transgene-free double mutants (*atals ataac2*) and single mutants (*atals* or *ataac2*) were readily identified in the standard T_2 lines (Fig. 3g and Extended Data Fig. 6b). As expected, the T_3 generation from three T_2 lines (nos. 14-23, 17-11 and 17-22) all showed herbicide resistance, conferred by base-edited *AtALS* alleles (Fig. 3h and Supplementary Fig. 2a). Consistently, NGS-based genotype analysis of two T_3 populations showed high-frequency base editing at *AtALS* and *AtACC2* sites (Supplementary Fig. 2b,c).

We investigated whether the Cas9-Act3.0-A + GE and CBE-Cas9n-Act3.0-A + BE constructs would induce potential off-target events at *AtFT* target sites with a 15-nt protospacer. Among a total of 184 selected T_2 extra-early flowering plants and transgene-free plants, no off-target event was detected at both *AtFT* sites for either Cas9-Act3.0 or CBE-Cas9n-Act3.0 systems (Extended Data Fig. 7a,b). Altogether, we developed a highly specific CRISPR-Combo-based pipeline for rapid generation of transgene-free genome-edited plants (Fig. 3i).

Accelerated regeneration of genome-edited poplar. Many plant species and cultivars are recalcitrant to tissue culture and regeneration, hindering genome editing applications[33]. To overcome this challenge, ectopic expression of morphogenic genes could be applied to boost plant tissue culture and de novo meristem regeneration[34–36]. Given the pluripotency potential of plant cells and the presence of morphogenic genes in every plant genome, we hypothesize that plant regeneration could be stimulated by activation of endogenous morphogenic genes. We first explored this idea in poplar, a woody plant and bioenergy crop. A CRISPR-Combo construct was made to simultaneously edit *Pt4CL1* and activate the poplar morphogenic gene *WUSCHEL* (*PtWUS*)[37] (Supplementary Table 1) and the Cas9 was driven by a strong constitutive promoter AtUBQ10. Compared to the conventional Cas9-GE construct, the CRISPR-Combo construct (Cas9-Act3.0-A + GE) resulted in accelerated root initiation and shoot growth in two independent experiments (Fig. 4a and Extended Data Fig. 8a). With CRISPR-Combo, the days to root were reduced by half while the rooting rate doubled to nearly 100% (Fig. 4b and Extended Data Fig. 8a). Expression analysis by quantitative reverse-transcription PCR (qRT–PCR) on 20 CRISPR-Combo T_0 lines showed *PtWUS* activation for the majority of lines, with activation in multiple lines in excess of 100-folds (Fig. 4c). Remarkably, both Cas9 and CRISPR-Combo systems resulted in 100% genome editing efficiency and >75% of lines carried homozygous or biallelic mutations for either construct (Fig. 4d and Extended Data Fig. 8b). We further tested three CRISPR-Combo lines with various levels of *PtWUS* activation on the callus induction medium (CIM). Interestingly, the lines (nos. 2 and 4) with 200-fold or higher *PtWUS* activation showed very rapid de novo callus induction from petiole cuttings, when compared to the low activation line (no. 17) or the control line (Extended Data Fig. 8c). We also conducted de novo callus regeneration from leaf discs and observed that more calli were induced from leaf discs of *PtWUS* high-activation lines (nos. 2 and 4) (Extended Data Fig. 8c). Interestingly, *PtWUS* high-activation lines nos. 4 and 2 showed more robust de novo root initiation and shoot growth of stem cuttings and the resulting in vitro cultured plants outgrew the controls in size (Fig. 4e and Extended Data Fig. 8d,e). Importantly, the *PtWUS* high-activation line (no. 4) grown in soil showed significantly increased plant height ($P = 0.025$) and substantially enhanced shoot biomass ($P = 0.054$) (Fig. 4f). The root length and biomass were also predominantly increased ($P = 0.035$ and $P = 0.013$) (Fig. 4g). Compared to control lines, the leaf area of line no. 4 was on average enlarged by 25% (Extended Data Fig. 8g). Enhanced shoot and root growth were also observed in line no. 2 but this was not statistically significant (Extended Data Fig. 8f-h). Overall, these results suggest that CRISPR-Combo enables rapid generation and propagation of genome-edited poplar by activating *PtWUS*.

We decided to test a second gene, *PtWOX11* (ref. [38]), for promoting poplar tissue culture. Again, *Pt4CL1* is the genome editing target in this CRISPR-Combo construct. Analysis of ten randomly chosen CRISPR-Combo T_0 lines showed high level of *PtWOX11* activation with some lines showing up to 800-fold (Fig. 4h). Importantly, *Pt4CL1* was edited in all these ten T_0 lines, with one heterozygous mutant, four biallelic mutants and five mosaic mutants (Fig. 4i). Analysis of the biallelic and heterozygous mutants showed mutations of 1 base pair insertion of A or T at the target site (Extended Data Fig. 9a). Interestingly, like the *PtWUS* high-activation lines,

Fig. 3 | CRISPR-Combo systems enable rapid breeding of transgene-free genome-edited plants by promoting flowering. a, Representative images of CRISPR-Combo-mediated T_1 *Arabidopsis* plants. Early flowering phenotype is observed in both Cas9-Act3.0-A + GE and CBE-Cas9n-Act3.0-A + BE T_1 populations. Two gR2.0 with 15-nt protospacers were used for *AtFT* activation. One gR1.0 each with a 20-nt protospacer was used for genome editing of *AtPYL1, AtAP1, AtALS* and *AtACC2*. Black arrows indicate extra-early flowering plants. The T_1 *Arabidopsis* plants were grown on the MS medium with hygromycin selection. **b**,**c**, Determination of the efficiency of indel mutation (**b**) and C to T conversion (**c**) from T_1 extra-early, early and standard flowering plants using NGS. The flowering phenotypes (extra-early, early and standard) were defined on the basis of the rosette leaf number when flower buds became visible. A total of 53 and 48 independent plants are examined for **b** and **c**, respectively. Box plots, 25th–75th percentile; centre line, median; whiskers, full data range in **b** and **c**. *P* values were obtained using the two-tailed Student's *t*-test. $^*P < 0.05$, $^{**}P < 0.01$. **d**, Representative images of T_2 progenies of T_1 extra-early flowering plants. **e**,**f**, Segregation pattern of flowering phenotype and T-DNA integration for T_2 Cas9-Act3.0-A + GE (**e**) and CBE-Cas9n-Act3.0-A + BE (**f**) populations. A total of six T_1 independent extra-early flowering transgenic lines are examined for both systems. The progenies resulting from the self-pollination of the selected extra-early flowering lines are classified into extra-early flowering, early flowering and standard flowering plants. The T-DNA integration was identified among the T_2 standard flowering plants by PCR method. vs, versus. **g**, Representative genotypes of *atals atacc2* in T_2 T-DNA free standard flowering populations. The DNA bases C in the protospacer sequence are highlighted in red. The numbers below the protospacer sequence indicate the percentage of DNA base T or C in total reads analysed by the CRISPR RGEN tools. **h**, Phenotype of the T_3 progeny of *atals atacc2* grown on the MS medium containing 1 mg l^{-1} of tribenuron. Representative lines of nos. 17-11, 17-22 and 14-23 are shown. WT, wild type. **i**, Diagram of CRISPR-Combo system-mediated rapid breeding of transgene-free edited plants. A, activation; GE, genome editing; BE, base editing.

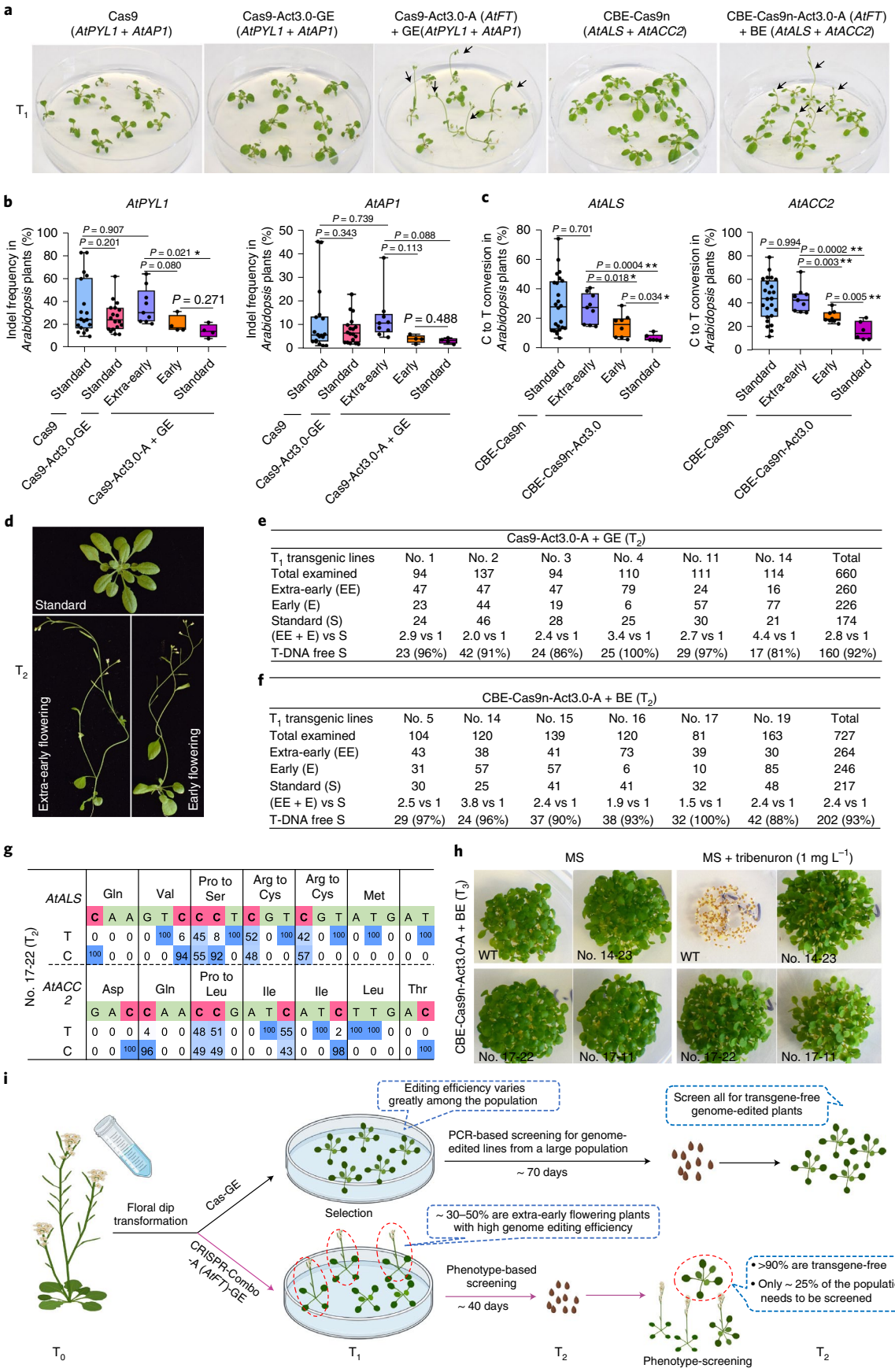

e	Cas9-Act3.0-A + GE (T_2)						
T_1 transgenic lines	No. 1	No. 2	No. 3	No. 4	No. 11	No. 14	Total
Total examined	94	137	94	110	111	114	660
Extra-early (EE)	47	47	47	79	24	16	260
Early (E)	23	44	19	6	57	77	226
Standard (S)	24	46	28	25	30	21	174
(EE + E) vs S	2.9 vs 1	2.0 vs 1	2.4 vs 1	3.4 vs 1	2.7 vs 1	4.4 vs 1	2.8 vs 1
T-DNA free S	23 (96%)	42 (91%)	24 (86%)	25 (100%)	29 (97%)	17 (81%)	160 (92%)

f	CBE-Cas9n-Act3.0-A + BE (T_2)						
T_1 transgenic lines	No. 5	No. 14	No. 15	No. 16	No. 17	No. 19	Total
Total examined	104	120	139	120	81	163	727
Extra-early (EE)	43	38	41	73	39	30	264
Early (E)	31	57	57	6	10	85	246
Standard (S)	30	25	41	41	32	48	217
(EE + E) vs S	2.5 vs 1	3.8 vs 1	2.4 vs 1	1.9 vs 1	1.5 vs 1	2.4 vs 1	2.4 vs 1
T-DNA free S	29 (97%)	24 (96%)	37 (90%)	38 (93%)	32 (100%)	42 (88%)	202 (93%)

the lines (nos. 2, 3 and 6) with 600-fold or higher *PtWOX11* activation also showed rapid de novo callus regeneration from petiole cuttings (Extended Data Fig. 9b), resulting in more adventitious shoots per explant (Fig. 4j). The regenerated shoots from *PtWOX11*-activation lines (nos. 2, 3 and 6) showed faster rooting than those from control plants in rooting medium (Extended Data Fig. 9c). As expected, compared to control plants, soil-grown plants (nos. 2, 3 and 6) showed increased root length and root biomass production (Fig. 4k). The plant height, shoot biomass and leaf area were also increased, albeit without statistical significance for most tested lines (Extended Data Fig. 9d).

In another case, we targeted *PtARK1* (ref. [39]) for activation. Analysis of ten CRISPR-Combo T_0 lines showed *PtARK1* activation in all lines, ranging from 25- to 80-fold (Supplementary Fig. 3a). A total of 70% of the T_0 lines were genome-edited at the *Pt4CL1* site (Supplementary Fig. 3b,c). Although this CRISPR-Combo construct also worked well, we did not observe any clear improvement of poplar tissue culture with *PtARK1* activation (data not shown). Taken together, these results demonstrated a CRISPR-Combo-based approach for enhanced adventitious shoot and root regeneration as well as robust in vitro propagation of genome-edited poplar plants by activation of the morphogenic genes *PtWUS* and *PtWOX11*.

Enhanced rice regeneration and genome editing. We reasoned that CRISPR-Combo-based morphogenic gene activation could also be applied to boost regeneration of annual plants. To this end, we applied CRISPR-Combo in rice by simultaneous genome editing (at *OsGW2* and *OsGN1a*) and gene activation of *OsBBM1*, a morphogenic gene that was previously reported as a trigger for embryogenic development[40]. The Cas9 was driven by a strong constitutive promoter ZmUbi. Activation of *OsBBM1* by CRISPR-Combo greatly improved regeneration of *Agrobacterium*-transformed rice callus (Fig. 5a). Compared to the no-activation control construct (Cas9-Act3.0-GE), the CRISPR-Combo construct (Cas9-Act3.0-A + GE) resulted in higher numbers of transformed calli, which translated to more regenerated plants (Fig. 5a,b and Extended Data Fig. 10a,b). The CRISPR-Combo construct also resulted in significantly more transgenic plants per callus (Fig. 5c). Interestingly, NGS-based genotypic analysis showed that the activation of *OsBBM1* resulted in about twice as many germline-transmittable mutations (homozygous, biallelic and heterozygous) as the non-activation construct at the *OsGW2* target site (Fig. 5d,e and Supplementary Fig. 4). A similar result was also identified at the *OsGN1a* target site (Extended Data Fig. 10c and Supplementary Fig. 5).

Inspired by these results, we sought to develop a method that can enrich high-efficiency genome-edited plants through morphogenic gene activation. Rice culture medium typically contains plant hormones auxin and cytokinin, which promote plant regeneration through inducing the expression of key morphogenic genes. Since expression of *OsBBM1* in rice egg cells is sufficient to reprogramme embryo formation[40], we reasoned that activation of *OsBBM1* in rice callus may be sufficient to render plant regeneration without exogenously supplying auxin and cytokinin. Impressively, it was indeed the case as *OsBBM1* activation led to regeneration of transformed calli and seedlings in the hormone-free (HF) culture medium in two independent experiments (Fig. 5f and Extended Data Fig. 10e), with an average of 35.7% callus transformation efficiency (Fig. 5g and Extended Data Fig. 10f). On average, two to five transgenic plants were produced per callus (Fig. 5h and Extended Data Fig. 10g). By contrast, without activation of *OsBBM1*, two hygromycin-resistant calluses from a total of 100 tested samples were occasionally generated and only one was able to regenerate into a rice plant (Fig. 5g and Extended Data Fig. 10f,g). Strikingly, all *OsGW2*-edited plants (89% of total plants) and *OsGN1a*-edited plants (66.5% of total plants) regenerated from the HF medium are homozygous, biallelic or heterozygous, except one chimaera at the *OsGN1a* target site (Fig. 5i,j, Extended Data Fig. 10h,i and Supplementary Fig. 6). The Combo rice plants regenerated in the HF manner showed normal phenotypes (Extended Data Fig. 10d,j). No off-target events were identified for either *OsGW2* or *OsGN1a* target sites in the plants regenerated in the HF manner (Supplementary Fig. 7). Furthermore, no cleavage activity of Cas9-Act3.0 was detected at the DNA-binding sites of *OsBBM1* promoter from the HF Combo plants (Extended Data Fig. 10k). Interestingly, we found that *OsBBM1* was not, or only slightly, activated in the HF Combo plants by analysing its messenger RNA level in mature leaves (Extended Data Fig. 10l), which suggests that the potential regulatory mechanism for tissue-specific downregulation of *OsBBM1* (ref. [40]) is largely intact in the CRISPR-Combo lines. Taken together, heritable targeted mutations by CRISPR-Combo were significantly enriched in the HF medium compared to the regular medium with hormones (Fig. 5d,i and Extended Data Fig. 10c,h).

In conclusion, we demonstrated that CRISPR-Combo can accelerate regeneration of genome-edited rice plants by activation of *OsBBM1* (Fig. 5k). More importantly, we developed an efficient method to enrich biallelic and monoallelic mutants over chimaeras through *OsBBM1* activation without the use of exogenous plant hormones after *Agrobacterium*-mediated transformation (Fig. 5k).

Discussion

We developed a new CRISPR-Combo platform to unleash versatile genome engineering in plants. The CRISPR-Combo systems allow for simultaneous genome editing and gene activation, which is conveniently achieved through guide RNA programming. Importantly, the CRISPR-Combo systems have an efficiency of editing and activation comparable to the corresponding single-function systems,

Fig. 4 | CRISPR-Combo systems enable rapid breeding of genome-edited plants by promoting regeneration in poplar. a, A Cas9-Act3.0 system promotes root initiation and shoot growth by activation of *PtWUS*. Two gR2.0 with 15-nt protospacers and one gR1.0 with 20-nt protospacer were used for *PtWUS* and *Pt4CL1*, respectively. All transgenic plants were grown in the root-induction medium (RIM) with hygromycin selection. **b**, The time and rate of root initiation. Upper graph: error bar, mean ± s.d. ($n = 5$–7 independent plants). Lower graph: error bar, mean ± s.d. ($n = 3$ biological replicates). The root initiation rate was evaluated on the seventh day after transgenic shoots were transferred to RIM. **c**,**h**, Determination of *PtWUS* (**c**) and *PtWOX11* (**h**) activation level in Cas9-Act3.0-mediated transgenic plants using qRT–PCR. Leaf tissue was sampled for total RNA extraction. CTRL, the randomly selected Cas9-mediated transgenic plant. Error bar, mean ± s.d. ($n = 3$ technical replicates). **d**,**i**, Zygosity analysis of Cas9- and Cas9-Act3.0-mediated T_0 *Pt4CL1* mutants. The frequencies of each zygotic type are shown as percentages. A total of 20 and 10 individual transgenic plants were examined in **d** and **i**, respectively. **e**, Cas9-Act3.0 promotes de novo root initiation of stem cuttings. Four stem cuttings were cultured in RIM. Red dashed circles indicate successful root initiation and white dashed circles indicate failed root initiation. **f**,**g**, Representative phenotype of shoot (**f**) and root (**g**) from CTRL and *PtWUS*-activation poplar line (no. 4). Plants were grown in soil under the same cultivation conditions for 6 weeks. Error bar, mean ± s.d. ($n = 4$ independent plants). **j**, Cas9-Act3.0 system promotes de novo shoot development of petiole cuttings by activation of *PtWOX11*. Petiole cuttings were cultured on the shoot-induction medium (SIM) for 20 d. The shoot number per explant was examined in a time series. Error bar, mean ± s.d. ($n = 3$ independent replicates). **k**, Representative phenotype of root from CTRL and *PtWOX11*-activation poplar lines. Plants were grown in soil under the same cultivation conditions for 6 weeks. Error bar, mean ± s.d. ($n = 4$ independent plants for CTRL, nos. 2 and 6; 3 independent plants for no. 3). *P* values in **b**,**f**,**g**,**k** were obtained using the two-tailed Student's *t*-test. $^*P < 0.05$, $^{**}P < 0.01$.

for example, CRISPR-Cas9, base editors and CRISPR-Act3.0. The high-efficiency and orthogonal functionalities of CRISPR-Combo hold great promise for a variety of applications in plants, as demonstrated in this study.

The generation time is one major bottleneck for genome editing-based plant breeding. Speed breeding can overcome this obstacle and is conventionally achieved using environmental manipulations[41]. Here we developed a genetic approach for speed breeding of genome-edited plants with CRISPR-Combo, through activation of a florigen *FT* (Fig. 3i). This new speed breeding technology offers three significant advantages over traditional breeding and genome editing methods. First, it significantly reduces the flowering time of genome-edited plants. Second, plants with high editing efficiency and without the transgene can be identified visually by phenotype-based screens in the first and second generations, respectively. Thus, it saves time and cost for molecular identification of genome-edited transgene-free plants. Third, it is very convenient to implement as it does not require a dedicated speed breeding growth chamber or room. Unlike many crops, floral dip transformation of egg cells is used to deliver the T-DNA and express

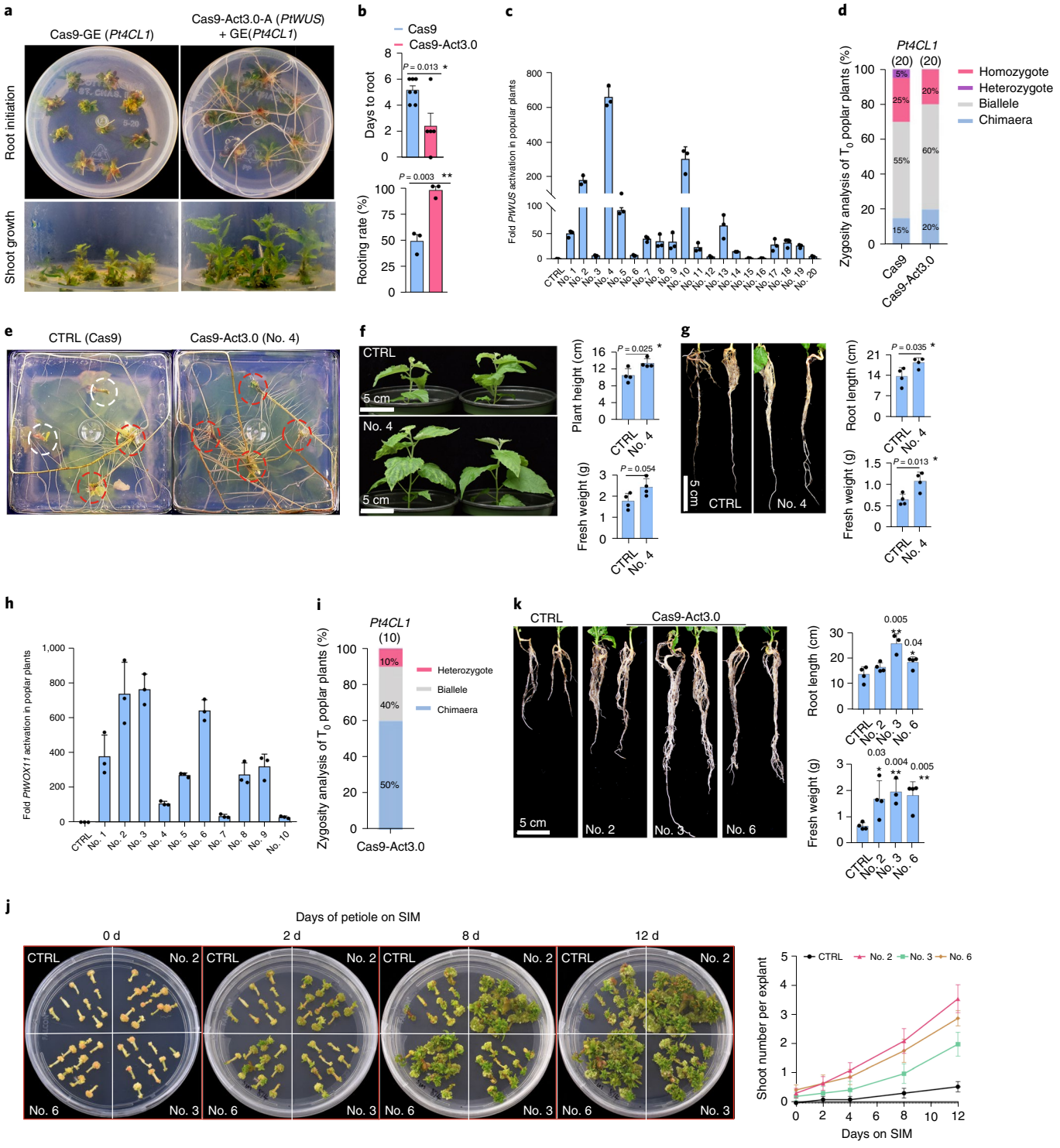

the transgene in *Arabidopsis*, which explains why egg cell-specific promoter was used to express Cas9 to generate heritable mutations in *Arabidopsis*[42]. In this regard, the use of constitutive promoter for CRISPR-Combo expression is probably not the best choice for *Arabidopsis*. However, such constitutive CRISPR-Combo systems should be readily transferable into crops as demonstrated by the efficient activation of a florigen in tomato (*SFT*) by CRISPR-Combo (Fig. 1d and Fig. 2d).

A second major challenge in plant genome editing is plant tissue culture and regeneration[33]. To boost the regeneration of genome-edited plants, exogenous developmental regulators and Cas9 reagents were typically constructed into independent expression cassettes and codelivered into plant cells[33–36]. By contrast, our CRISPR-Combo systems enable activation of the endogenous morphogenic genes by simply expressing targeting sgRNAs, which is more flexible and scalable, allowing for easy fine-tuning or multiplexed gene activation. Here we demonstrated the ability of CRISPR-Combo to promote plant regeneration in poplar and rice. In the bioenergy crop poplar, we showed that by simultaneous activation of endogenous morphogenic genes such as *PtWUS* and *PtWOX11*, regeneration of genome-edited plants could be accelerated. In addition, CRISPR-Combo promotes de novo callus and root organogenesis from petiole and stem cuttings, enabling rapid propagation of genome-edited poplar trees (Fig. 4 and Extended Data Figs. 8 and 9). Remarkably, shoot and root biomass production of these Combo lines were also enhanced (Fig. 4f,g,k). This technology could contribute to the development of improved poplar trees in the future carbon-neutral economy. In the staple crop rice, the regeneration of genome-edited plants can be accelerated by simultaneous activation of an endogenous morphogenic gene *OsBBM1*. Interestingly, a recent preprint reported that overexpression of *OsBBM1* resembled auxin-induced somatic embryogenesis in rice[43]. However, overexpression of *OsBBM1* using a strong DEX-inducible promoter was unable to achieve shoot regeneration of rice without exogenous supplement of plant hormone cytokinin[43]. In comparison, our success in achieving rice regeneration without exogenous plant hormones demonstrates that it may be advantageous to use CRISPR-Combo to overexpress an endogenous morphogenic gene to promote plant regeneration. Excitingly, this hormone-free method can significantly enrich heritable targeted mutations to create almost only biallelic and monoallelic mutants, indicating CRISPR-Combo-induced *OsBBM1* activation and target editing occurred in the same embryogenic cell. More remarkably, we have not observed clear developmental defects for CRISPR-Combo lines with activation of morphogenic genes in polar and rice. Conventional overexpression strategies of morphogenic genes completely remove the native promoter from the target gene, conferring robust ectopic expression in many tissues which leads to some negative consequences[34,43]. By contrast, gene activation systems just add one additional layer of transcriptional regulation without modifying the promoter sequence of the target gene, which does not necessarily help bypass or escape the transcriptional feedback regulation, as we previously found with CRISPR-Act2.0 and mTALE-Act systems[14]. The tissue-specific negative regulation of *OsBBM1* may be intact in the mature leaves of CRISPR-Combo lines, which helps prevent the negative effects if *OsBBM1* is constitutively activated. This may well be a great advantage of CRISPR-Combo for enabling plant tissue culture and genome editing. More future research on applying CRISPR-Combo in different crops to further test this hypothesis is warranted.

Another advantage of CRISPR-Combo is the positive correlation between genome editing and gene activation activities. Because both functionalities are achieved by a single Cas9 protein, high-efficiency genome-edited lines can be identified by using the phenotypes resulting from gene activation and vice versa. For example, CRISPR-Combo-generated extra-early flowering *Arabidopsis* plants had more robust genome-editing efficiency (Fig. 3b,c). The success in rice regeneration without the exogenous plant hormones must have relied on high levels of morphogenic gene activation, which explains why almost every single regenerated rice plant was genome edited (Fig. 5i). Thus, CRISPR-Combo-based hormone-free genome editing represents an efficient method to generate high-efficiency genome-edited plants. Since plant regeneration is strictly dependent on CRISPR component expression, nearly all regenerated plants in the hormone-free medium must be transgenic. Hence, this CRISPR-Combo-based method would potentially enable marker-free genome editing.

The demonstrated applications of CRISPR-Combo here are only the tip of the iceberg. CRISPR-Combo has many additional potential applications. For example, CRISPR-Combo can enable simultaneous activation of multiple morphogenic genes, which may be required to overcome the regeneration barrier of very recalcitrant crops. Also, CRISPR-Combo may be used to simultaneously activate a florigen gene and a morphogenic gene to further fast-track the breeding of transgene-free genome-edited crops. Furthermore, CRISPR-Combo may be used to promote certain genome editing outcomes by simultaneously activating a specific DNA-repair pathway. In addition, CRISPR-Combo may allow for sophisticated metabolic engineering or modulating signalling pathways which requires simultaneous gene editing and activation.

Fig. 5 | CRISPR-Combo enhances rice regeneration and facilitates recovery of heritable targeted mutations. a, Representative images of Cas9-Act3.0-mediated callus induction and shoot regeneration by activating *OsBMM1* in rice. Two gR2.0 with 15-nt protospacers were used for *OsBMM1* activation. One 20-nt protospacer each was used for genome editing of *OsGW2* and *OsGN1a*. GE, genome editing; A + GE, simultaneous gene activation and editing; RSM, rice selection medium; Reg I, regeneration I medium. All calli were subcultured with fresh medium every 2 weeks. The dashed white lines are used to separate two independent calli. **b**, Efficiency of Cas9-Act3.0-mediated callus induction and shoot regeneration. All calli were cultured under the same conditions. Hyg, hygromycin. **c**, Number of regenerated transgenic plants per Cas9-Act3.0-mediated callus. Each dot indicates the seedling number generated from one transgenic callus. Error bar, mean ± s.d. ($n = 10$ independent calli). *P* values were obtained using the two-tailed Student's *t*-test. **d**, Zygosity analysis of Cas9-Act3.0-mediated T_0 lines at the *OsGW2* target site. The frequencies of each zygotic type are shown as percentages. A total of 10 and 16 individual transgenic plants were examined for Cas9-Act3.0-based GE and A + GE vectors using NGS, respectively. **e**, Representative genotypes of Cas9-Act3.0-mediated T_0 mutants at the *OsGW2* site. The red dashes indicate a nucleotide deletion and the black dashes indicate a blank space. The bold DNA bases indicate insertion. PAM, protospacer adjacent motif. **f**, Representative images of Cas9-Act3.0-mediated hormone-free (HF) callus induction and regeneration by activating *OsBMM1* in rice. All calli were subcultured with fresh medium without any hormone every 2 weeks. **g**, Efficiency of Cas9-Act3.0-callus induction and regeneration in an HF manner. All calli were cultured under the same conditions. **h**, Number of regenerated transgenic plants per Cas9-Act3.0-mediated callus in an HF manner. Each dot indicates the seedling number generated from one transgenic callus. Error bar, mean ± s.d. ($n = 7$ independent calli). **i**, Zygosity analysis of Cas9-Act3.0-mediated T_0 *OsGW2OsGN1a* mutants in an HF manner. The frequencies of each zygotic type are shown as percentages ($n = 18$ transgenic plants). **j**, Representative genotypes of Cas9-Act3.0-mediated T_0 *OsGW2OsGN1a* mutants in an HF manner. The red dashes indicate a nucleotide deletion. The black dashes indicate a blank space. The bold DNA bases indicate insertion. **k**, Diagram of CRISPR-Combo system-mediated rapid breeding by promoting plant regeneration.

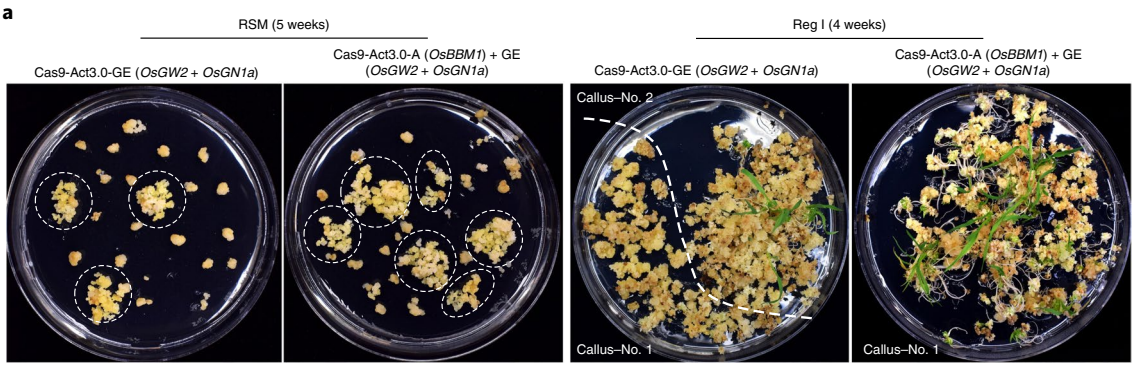

b

Callus	Cas9-Act3.0	
	GE	A + GE
Agro-infection	25	25
Hyg-resistance	12 (48%)	20 (80%)
Regeneration (2 weeks)	4 (33.3%)	18 (90%)
Regeneration (4 weeks)	9 (75%)	20 (100%)

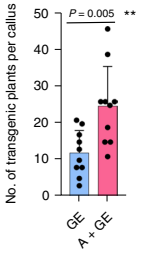

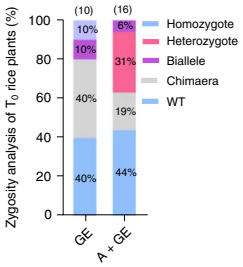

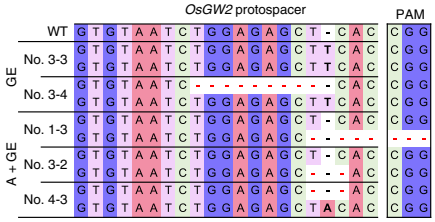

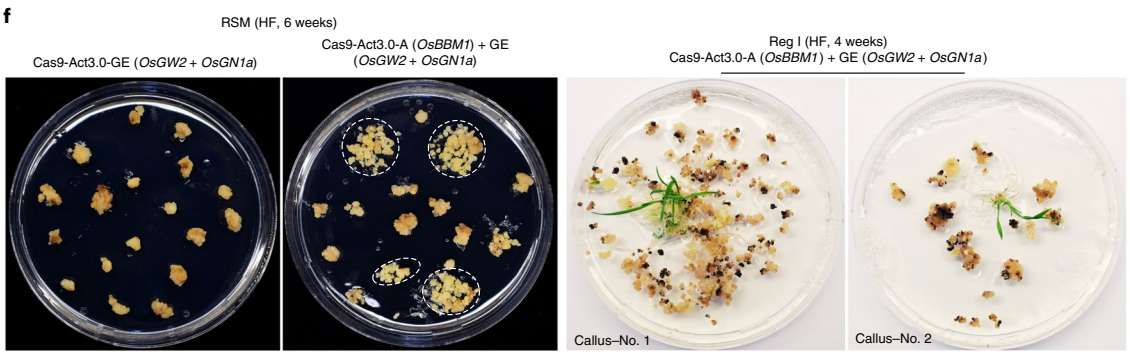

g

Callus	Cas9-Act3.0	
	GE	A + GE (HF)
Agro-infection	25	25
Hyg-resistance	0	10 (40%)
Regeneration (2 weeks)	0	6 (60%)
Regeneration (4 weeks)	0	8 (80%)

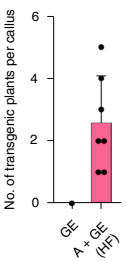

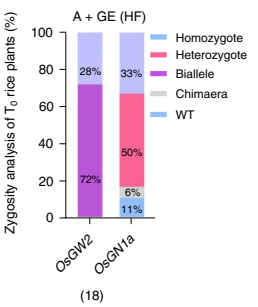

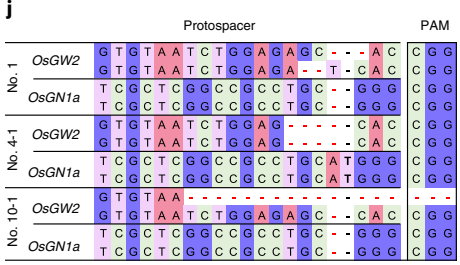

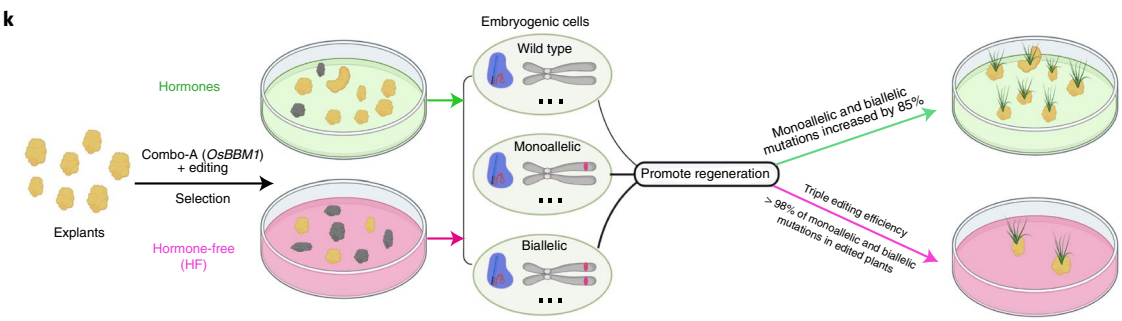

Recently, Cas9-based high-throughput functional genomic screens have been demonstrated in plants[18,19,44]. CRISPR-Combo could potentially enable combinational screens at the genome and transcriptome levels, opening another avenue into dissecting the relationship between genotype and phenotype in plants. Undoubtedly, the CRISPR-Combo platform will open new frontiers in plant genome engineering, metabolic engineering and synthetic biology.

Methods

Plant material and growth condition. Rice (*Oryza sativa* subspecies *japonica*) cultivar Kitaake, tomato cultivar Micro-Tom, *Arabidopsis thaliana* ecotype Columbia-0 (Col-0) and the hybrid poplar *Populus alba*×*tremula* clone 717-1B4 were used for protoplast assays or stable transformation in the study. Rice seedlings used for protoplast isolation were grown on MS medium at 28 °C in the dark for ~2 weeks. Transgenic plants of rice were grown in the greenhouse at around 29 °C with a 16 h-light/8 h-dark cycle. Tomato seedlings used for protoplast isolation were grown on MS medium with a 16 h-light/8 h-dark cycle at 25 °C for ~7 d. *Arabidopsis* plants were grown in a growth chamber with a 16 h-light/8 h-dark cycle at 22 °C. Transgenic plants of poplar were grown in a tissue culture chamber with a 24 h light condition at 25 °C.

Construction of CRISPR-Combo vectors. The detailed procedures for constructing Golden Gate sgRNA modular vectors and Gateway modular vectors for CRISPR-Combo are available in the Supplementary Methods. The oligos for sgRNA cloning are summarized in Supplementary Table 2.

Assembly of T-DNA expression vectors. The final T-DNA expression vectors were assembled by a Multisite Gateway cloning strategy with an attR1-attR2 destination vector pYPQ202 (Addgene no. 86198, for *Arabidopsis* and poplar), pYPQ203 (Addgene no. 86207, for rice) or pMDC32 (Addgene no. 32078, for tomato), an attL5-attL2 sgRNA expression entry clone and an attL1-attR5 Cas activator entry clone using Gateway LR clonase II (Invitrogen). The detailed procedure is described in the Supplementary Methods.

Rice and tomato protoplast transformation. Rice protoplast isolation and transformation were performed according to the previous report with minor modifications[23]. In tomato protoplast assays, the protoplast isolation and transformation followed the previous protocol with minor modifications[23,30]. Briefly, the protoplasts were first isolated from cotyledons of 8-day-old tomato seedlings using enzyme solution, resuspended in 0.55 M sucrose (pH 5.7) and then gently overlayed with 2 ml of W5 solution without mixing. Protoplast cells were collected from the interface between the W5 solutions and sucrose after the centrifugation of 30 min at 200*g*, washed with 10 ml of W5 solution and resuspended in MMG solution. To detect genome editing, plasmid DNA (20 μg per construct) was introduced into 180 μl of rice protoplasts (2×10^6 cells ml^{-1}) or tomato protoplasts (1×10^6 cells ml^{-1}) by PEG-mediated transfection. To determine the expression levels of targeted genes, plasmid DNA (40 μg per construct) was introduced into 360 μl of rice protoplasts (2×10^6 cells ml^{-1}) or tomato protoplasts (1×10^6 cells ml^{-1}) based on PEG-mediated transfection. The transfected rice and tomato protoplasts were incubated in the dark for 48 h at 32 and 28 °C, respectively, and then the protoplasts were collected for DNA or RNA extraction.

***Arabidopsis* stable transformation and phenotype analysis.** To generate *Arabidopsis* transgenic lines, *Agrobacterium tumefaciens* strain GV3101 containing T-DNA constructs was used for transformation of *Arabidopsis* plants via the floral dip method[23,45]. Seeds of T_0 to T_2 *Arabidopsis* plants were sterilized using 50% bleach with 0.05% Tween 20, washed five times with sterile water, vernalized at 4 °C in the dark for 2 d and then plated on MS plates containing hygromycin (15 μg ml^{-1}). After 7–10 d, transgenic plants were transferred to soil. The flowering phenotype (extra-early, early and standard) was defined on the basis of the number of rosette leaves when flower buds became visible. Extra-early flowering plants showed four leaves, early flowering plants showed ~6–18 leaves and standard flowering plants showed ~20–25 leaves when flower buds became visible. The number of flower buds were recorded every 3 d. The T-DNA region was detected using Phire Plant Direct PCR Kit (Thermo Fisher) by amplification of the CRISPR-Combo component.

Tribenuron resistance assay of *Arabidopsis* seeds. Seeds of wild-type and T_2 extra-early flowering plants were sterilized following the aforementioned method, vernalized at 4 °C in the dark for 2 d and then plated on MS-hygromycin plates containing different concentrations of tribenuron (0, 1, 2.5 and 5 mg l^{-1}). After ~10 d, the tested *Arabidopsis* seeds and seedlings were photographed.

Poplar stable transformation. To generate poplar transgenic plants, *Populus alba*×*tremula* clone 717-1B4 was used for stable transformation following the previous method[46] with minor modifications. The T-DNA constructs were transformed into the *A. tumefaciens* strain GV3101. Transgenic shoots regenerated from explants were cultured on a shoot-induction medium containing 20 μg ml^{-1} of hygromycin. The regenerated shoots at a height of 1–2 cm were transferred to a root-induction medium containing 20 μg ml^{-1} of hygromycin. Rooted plants were propagated and used for genotyping. To test the de novo callus and root organogenesis of *PtWUS*- and *PtWOX11*-activation plants, the petiole, leaf disc, stem cuttings or regenerated shoots sampled from the *PtWUS*- and *PtWOX11*-activation plants were cultured with callus-, shoot- or root-induction media. Explants were subcultured with fresh medium every 2 weeks. A ruler was used to measure the height and root length of transgenic poplar plants. To analyse the average area of poplar leaves, the total area of all leaves of each plant was measured using LI-3100C Area Meter (LI-COR) and then divided by the number of tested leaves.

Rice stable transformation. To generate transgenic rice plants, the *A. tumefaciens* strain EHA105 containing T-DNA constructs was used for the transformation of Kitaake callus cells as previously reported[23]. On the basis of this method, 2 μg ml^{-1} of 2,4-D was supplied into coculture medium and selection medium, and 1 μg ml^{-1} of NAA and 2 μg ml^{-1} of kinetin were supplied into regeneration I medium. To test the efficiency of CRISPR-Combo-mediated callus and shoot regeneration in the hormone-free manner, no hormone was supplied into the rice coculture medium, selection medium or regeneration I medium.

Genotyping of transgenic rice plants. NGS was used to detect the mutations of genome-edited rice plants. These edited rice plants were categorized into five genotypes including biallelic, homozygous, heterozygous, chimaeric and wild-type following these criteria: biallelic, total mutation frequency ≥70% with each of two major types ≥30%; homozygous, one type of mutation ≥70%; heterozygous, one type of mutation ≥30% but total mutation frequency <70%; chimaeric, 15% ≤ total mutation frequency < 30%; wild-type, total mutation frequency <15%.

Restriction fragment length polymorphism analysis. The RFLP method was used to analyse the mutation efficiency in some rice protoplasts assays. Briefly, the targeted genomic regions were amplified by PCR following the instructions of Phire Plant Direct PCR Kit (Thermo Fisher), then verified by gel electrophoresis. PCR products were purified with QIAQuick PCR Purification Kit (QIAGEN) and quantified by Nanodrop (Thermo Fisher) and then digested with specific restriction enzymes using equal amounts of PCR amplicons for each sample. Digested PCR products were visualized on 2% TAE (Tris-acetate-EDTA) agarose gels. Mutation efficiencies were quantified using Image Lab Software (Bio-Rad Laboratories) on the basis of band intensity.

Mutation analysis by next-generation sequencing. NGS was used to analyse genome editing results in this study. For protoplasts assays, the targeted genomic regions were directly amplified from protoplast cells following the instructions of Phire Plant Direct PCR Kit (Thermo Fisher) and barcoded using the Hi-TOM primers[47]. For stable transgenic plants, DNA was extracted from leaf tissue using CTAB method[48] and barcoded using the Hi-TOM primers. PCR products were verified by gel electrophoresis. Around 6–60 PCR products were pooled together and purified with QIAQuick PCR Purification Kit (QIAGEN) and then quantified by Nanodrop (Thermo Fisher). The purified PCR products were used for Illumina HiSeq2500 sequencing. For targeted mutagenesis, the NGS data were analysed with CRISPRMatch[49] and CRISPResso2 (ref. [50]). For base editing, the NGS data were analysed with CRISPR RGEN Tools (http://www.rgenome.net/be-analyzer/#!).

RNA extraction and qPCR analysis. For protoplast assays, the total RNA was extracted from ~$1–5\times10^5$ rice or tomato protoplast cells using TRIzol reagent (Thermo Fisher) on the basis of the manufacturer's instructions[23]. For poplar and rice plants, total RNA was extracted using the RNeasy Plant Mini Kit (QIAGEN). Then, DNase I (RNase-free) (New England Biolabs) was used to remove DNA from the total RNA samples. Approximately 500–1,000 ng of total RNA was used for complementary DNA synthesis with the SuperScript III First-Strand Synthesis Kit (Thermo Fisher). The AzuraQuant Green Fast qPCR Mix (Azura Genomics) coupled with the CFX96 Touch Real-Time PCR Detection System (Bio-Rad) was used to detect the transcript expression levels of target genes. *OsTubulin* and *SlUbi3* were used as the endogenous control gene for rice and tomato, respectively. Both *PtCDC2* and *PtPT1* were selected as the endogenous control genes for poplar. The fold changes of target genes were calculated by the $2^{-\Delta\Delta Ct}$ method. All primers used in this study are listed in Supplementary Table 3.

Reporting Summary. Further information on research design is available in the Nature Research Reporting Summary linked to this article.

Data availability

All generated and processed data from this study are included in the published article and its Supplementary Information. The Golden Gate and Gateway compatible vectors for the CRISPR-Combo systems were deposited to Addgene: pYPQ-Cas9-Act3.0 (no. 178954), pYPQ-CBE-Cas9n-Act3.0 (no. 178955), pYPQ-ABE-Cas9n-Act3.0 (no. 178956), pYPQ-SpRY-Act3.0 (no. 178957), pYPQ-CBE-SpRYn-Act3.0 (no. 178958), pYPQ-ABE-SpRYn-Act3.0 (no.

178959), pYPQ-132-tRNA (no. 179211), pYPQ-133-tRNA (no. 179212), pYPQ-134-tRNA (no. 179213) and pYPQ-134B (no. 179216). The sequence data of targeted genes can be found from The Arabidopsis Information Resource (https://www.Arabidopsis.org/), Rice Genome Annotation Project (http://rice.uga.edu/) Solanaceae Genomics Network (https://solgenomics.net/) or Phytozome (https://phytozome-next.jgi.doe.gov/) using their locus identifiers as follows: *OsBBM1* (LOC_Os11g19060), *OsGW2* (LOC_Os02g14720), *OsGN1a* (LOC_Os01g10110), *OsALS* (LOC_Os02g30630), *OsEPSPS* (LOC_Os06g04280), *OsYSA* (LOC_Os03g40020), *OsMAPK5* (LOC_Os03g17700), *AtFT* (AT1G65480), *AtAP1* (AT1G69120), *AtPYL1* (AT5G46790), *AtALS* (AT3G48560), *AtACC2* (AT1G36180), *PtWUS* (Potri.005G114700), *PtWOX11* (Potri.013G066900), *PtARK1* (Potri.011G011100), *Pt4CL1* (Potri.001G036900), *SFT* (Solyc03g063100) and *SolyA7* (Solyc01g010970). The NGS data have been deposited to National Center for Biotechnology Information (accession code PRJNA779678; https://www.ncbi.nlm.nih.gov/bioproject/PRJNA779678).

Received: 17 December 2021; Accepted: 11 April 2022;
Published online: 20 May 2022

References

1. Jinek, M. et al. A programmable dual-RNA-guided DNA endonuclease in adaptive bacterial immunity. *Science* **337**, 816–821 (2012).
2. Zhang, Y., Malzahn, A. A., Sretenovic, S. & Qi, Y. The emerging and uncultivated potential of CRISPR technology in plant science. *Nat. Plants* **5**, 778–794 (2019).
3. Gao, C. Genome engineering for crop improvement and future agriculture. *Cell* **184**, 1621–1635 (2021).
4. Anzalone, A. V., Koblan, L. W. & Liu, D. R. Genome editing with CRISPR-Cas nucleases, base editors, transposases and prime editors. *Nat. Biotechnol.* **38**, 824–844 (2020).
5. Molla, K. A., Sretenovic, S., Bansal, K. C. & Qi, Y. Precise plant genome editing using base editors and prime editors. *Nat. Plants* **7**, 1166–1187 (2021).
6. Grunewald, J. et al. A dual-deaminase CRISPR base editor enables concurrent adenine and cytosine editing. *Nat. Biotechnol.* **38**, 861–864 (2020).
7. Zhang, X. et al. Dual base editor catalyzes both cytosine and adenine base conversions in human cells. *Nat. Biotechnol.* **38**, 856–860 (2020).
8. Sakata, R. C. et al. Base editors for simultaneous introduction of C-to-T and A-to-G mutations. *Nat. Biotechnol.* **38**, 865–869 (2020).
9. Li, C. et al. Targeted, random mutagenesis of plant genes with dual cytosine and adenine base editors. *Nat. Biotechnol.* **38**, 875–882 (2020).
10. Li, C. et al. SWISS: multiplexed orthogonal genome editing in plants with a Cas9 nickase and engineered CRISPR RNA scaffolds. *Genome Biol.* **21**, 141 (2020).
11. Maeder, M. L. et al. CRISPR RNA-guided activation of endogenous human genes. *Nat. Methods* **10**, 977–979 (2013).
12. Perez-Pinera, P. et al. RNA-guided gene activation by CRISPR-Cas9-based transcription factors. *Nat. Methods* **10**, 973–976 (2013).
13. Lowder, L. G. et al. A CRISPR/Cas9 toolbox for multiplexed plant genome editing and transcriptional regulation. *Plant Physiol.* **169**, 971–985 (2015).
14. Lowder, L. G. et al. Robust transcriptional activation in plants using multiplexed CRISPR-Act2.0 and mTALE-act systems. *Mol. Plant* **11**, 245–256 (2018).
15. Pan, C., Sretenovic, S. & Qi, Y. CRISPR/dCas-mediated transcriptional and epigenetic regulation in plants. *Curr. Opin. Plant Biol.* **60**, 101980 (2021).
16. Esvelt, K. M. et al. Orthogonal Cas9 proteins for RNA-guided gene regulation and editing. *Nat. Methods* **10**, 1116–1121 (2013).
17. Boettcher, M. et al. Dual gene activation and knockout screen reveals directional dependencies in genetic networks. *Nat. Biotechnol.* **36**, 170–178 (2018).
18. Bai, M. et al. Generation of a multiplex mutagenesis population via pooled CRISPR-Cas9 in soya bean. *Plant Biotechnol. J.* **18**, 721–731 (2020).
19. Liu, H. J. et al. High-throughput CRISPR/Cas9 mutagenesis streamlines trait gene identification in maize. *Plant Cell* **32**, 1397–1413 (2020).
20. Kiani, S. et al. Cas9 gRNA engineering for genome editing, activation and repression. *Nat. Methods* **12**, 1051–1054 (2015).
21. Singh, D. et al. Real-time observation of DNA target interrogation and product release by the RNA-guided endonuclease CRISPR Cpf1 (Cas12a). *Proc. Natl. Acad. Sci. USA* **115**, 5444–5449 (2018).
22. Breinig, M. et al. Multiplexed orthogonal genome editing and transcriptional activation by Cas12a. *Nat. Methods* **16**, 51–54 (2019).
23. Pan, C. et al. CRISPR-Act3.0 for highly efficient multiplexed gene activation in plants. *Nat. Plants* **7**, 942–953 (2021).
24. Walton, R. T., Christie, K. A., Whittaker, M. N. & Kleinstiver, B. P. Unconstrained genome targeting with near-PAMless engineered CRISPR-Cas9 variants. *Science* **368**, 290–296 (2020).
25. Ren, Q. et al. PAM-less plant genome editing using a CRISPR-SpRY toolbox. *Nat. Plants* **7**, 25–33 (2021).
26. Ren, J. et al. Expanding the scope of genome editing with SpG and SpRY variants in rice. *Sci. China Life Sci.* **64**, 1784–1787 (2021).
27. Xu, Z. et al. SpRY greatly expands the genome editing scope in rice with highly flexible PAM recognition. *Genome Biol.* **22**, 6 (2021).
28. Ren, Q. et al. Improved plant cytosine base editors with high editing activity, purity, and specificity. *Plant Biotechnol. J.* **19**, 2052–2068 https://doi.org/10.1111/pbi.13635 (2021).
29. Li, G., Sretenovic, S., Eisenstein, E., Coleman, G. & Qi, Y. Highly efficient C-to-T and A-to-G base editing in a *Populus* hybrid. *Plant Biotechnol. J.* https://doi.org/10.1111/pbi.13581 (2021).
30. Randall, L. B. et al. Genome- and transcriptome-wide off-target analyses of an improved cytosine base editor. *Plant Physiol.* https://doi.org/10.1093/plphys/kiab264 (2021).
31. Richter, M. F. et al. Phage-assisted evolution of an adenine base editor with improved Cas domain compatibility and activity. *Nat. Biotechnol.* **38**, 883–891 (2020).
32. Lapinaite, A. et al. DNA capture by a CRISPR-Cas9-guided adenine base editor. *Science* **369**, 566–571 (2020).
33. Altpeter, F. et al. Advancing crop transformation in the era of genome editing. *Plant Cell* **28**, 1510–1520 (2016).
34. Lowe, K. et al. Morphogenic regulators *Baby boom* and *Wuschel* improve monocot transformation. *Plant Cell* https://doi.org/10.1105/tpc.16.00124 (2016).
35. Maher, M. F. et al. Plant gene editing through de novo induction of meristems. *Nat. Biotechnol.* **38**, 84–89 (2020).
36. Debernardi, J. M. et al. A GRF-GIF chimeric protein improves the regeneration efficiency of transgenic plants. *Nat. Biotechnol.* **38**, 1274–1279 (2020).
37. Li, J. et al. The WUSCHELa (PtoWUSa) is involved in developmental plasticity of adventitious root in poplar. *Genes* **11**, https://doi.org/10.3390/genes11020176 (2020).
38. Liu, B. et al. *PtWOX11* acts as master regulator conducting the expression of key transcription factors to induce de novo shoot organogenesis in poplar. *Plant Mol. Biol.* **98**, 389–406 (2018).
39. Liu, X., Zhang, Z., Bian, W., Duan, A. & Zhang, H. Enhancing the expression of ARK1 genes in poplar leads to multiple branches and transcriptomic changes. *R. Soc. Open Sci.* **7**, 201201 (2020).
40. Khanday, I., Skinner, D., Yang, B., Mercier, R. & Sundaresan, V. A male-expressed rice embryogenic trigger redirected for asexual propagation through seeds. *Nature* **565**, 91–95 (2019).
41. Watson, A. et al. Speed breeding is a powerful tool to accelerate crop research and breeding. *Nat. Plants* **4**, 23–29 (2018).
42. Wang, Z. P. et al. Egg cell-specific promoter-controlled CRISPR/Cas9 efficiently generates homozygous mutants for multiple target genes in *Arabidopsis* in a single generation. *Genome Biol.* **16**, 144 (2015).
43. Khanday, I., Santos-Medellín, C. & Sundaresan, V. Rice embryogenic trigger BABY BOOM1 promotes somatic embryogenesis by upregulation of auxin biosynthesis genes. *bioRxiv* https://doi.org/10.1101/2020.08.24.265025 (2020).
44. Meng, X. et al. Construction of a genome-wide mutant library in rice using CRISPR/Cas9. *Mol. Plant* https://doi.org/10.1016/j.molp.2017.06.006 (2017).
45. Clough, S. J. & Bent, A. F. Floral dip: a simplified method for *Agrobacterium*-mediated transformation of *Arabidopsis thaliana*. *Plant J.* **16**, 735–743 (1998).
46. Leple, J. C., Brasileiro, A. C., Michel, M. F., Delmotte, F. & Jouanin, L. Transgenic poplars: expression of chimeric genes using four different constructs. *Plant Cell Rep.* **11**, 137–141 (1992).
47. Liu, Q. et al. Hi-TOM: a platform for high-throughput tracking of mutations induced by CRISPR/Cas systems. *Sci. China Life Sci.* **62**, 1–7 (2019).
48. Stewart, C. N. Jr. & Via, L. E. A rapid CTAB DNA isolation technique useful for RAPD fingerprinting and other PCR applications. *Biotechniques* **14**, 748–750 (1993).
49. You, Q. et al. CRISPRMatch: an automatic calculation and visualization tool for high-throughput CRISPR genome-editing data analysis. *Int. J. Biol. Sci.* **14**, 858–862 (2018).
50. Clement, K. et al. CRISPResso2 provides accurate and rapid genome editing sequence analysis. *Nat. Biotechnol.* **37**, 224–226 (2019).

Acknowledgements

This work was supported by the NSF Plant Genome Research Program grants (award nos. IOS-1758745 and IOS-2029889), the USDA-NIFA Biotechnology Risk Assessment grant (award no. 2020-33522-32274), the USDA-AFRI Agricultural Innovations Through Gene Editing Program (award no. 2021-67013-34554) and Maryland Innovation Initiative Funding (award no. 1120-012_2) to Y.Q. and a USDA-NIFA grant (award no. 2019-67013-29197) and a USDA McIntire-Stennis project (award no. MD-PSLA-20006) to G.C. A.M. was supported by NRT-INFEWS: UMD Global STEWARDS (STEM Training at the Nexus of Energy, Water Reuse and Food Systems) that was awarded to the University of Maryland School of Public Health by the NSF National Research Traineeship Program (award no. 1828910). S.S. is a fellow of Foundation for Food and Agriculture Research.

Author contributions

Y.Q. and C.P. conceived the project and designed the experiments. C.P., B.L. and S.S. generated all the constructs. C.P. and Y.C. performed all experiments of rice and tomato. A.M. generated stable transgenic *Arabidopsis*. C.P. conducted molecular and phenotype analysis on these lines. G.L. and G.C. generated stable poplar plants and conducted the analysis. F.G. provided help during stable transformation of rice. Y.Q. and C.P. wrote the paper with input from other authors. All authors read and approved the final manuscript.

Competing interests

Y.Q. and C.P. are inventors on a US Patent Application that has been filed on the CRISPR-Combo system in this study. Y.Q. is a consultant for Inari Agriculture and CTC Genomics. All other authors declare no competing interests.

Additional information

Extended data is available for this paper at https://doi.org/10.1038/s41477-022-01151-9.

Supplementary information The online version contains supplementary material available at https://doi.org/10.1038/s41477-022-01151-9.

Correspondence and requests for materials should be addressed to Yiping Qi.

Peer review information *Nature Plants* thanks Jian-feng Li, Sadiye Hayta and the other, anonymous, reviewer(s) for their contribution to the peer review of this work.

Reprints and permissions information is available at www.nature.com/reprints.

Publisher's note Springer Nature remains neutral with regard to jurisdictional claims in published maps and institutional affiliations.

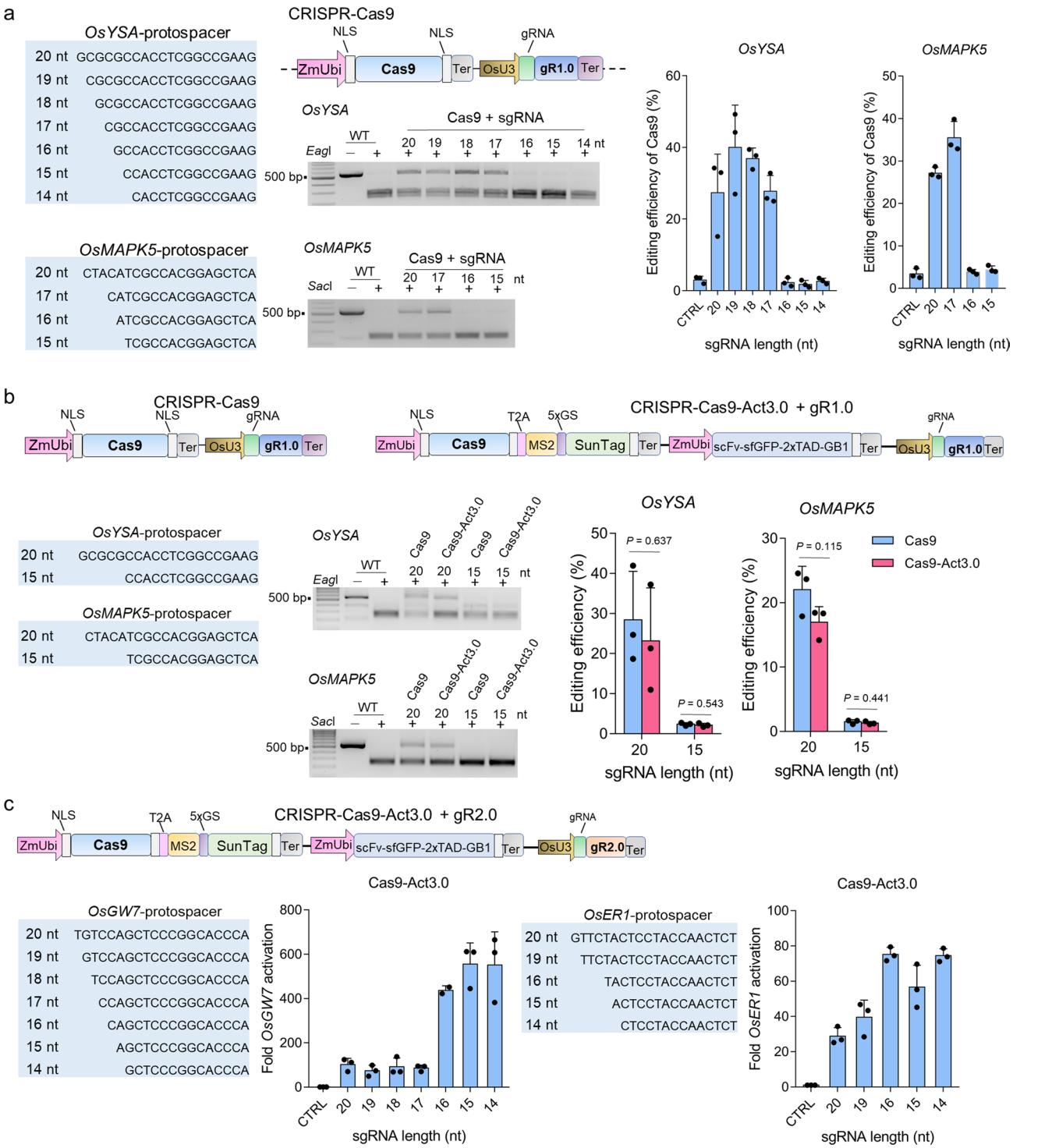

Extended Data Fig. 1 | CRISPR-Cas9-Act3.0 enables genome editing and gene activation in rice protoplasts programmed by guide RNA scaffolds and protospacer length. a, Restriction fragment length polymorphism (RFLP) analysis of CRISPR-Cas9-mediated genome editing with different protospacer length (14-nt to 20-nt) in gR1.0. The Cas9 and single guide (sgRNA) scaffold gR1.0 were driven by ZmUbi and OsU3 promoters, respectively. Three biological replicates were performed for each target site. Representative gel images are shown. CTRL indicates wild-type samples. Each dot represents an individual biological replicate. Error bar represents the mean ± s.d. (n = 3 independent experiments). NLS, nuclear localization signal. **b**, Comparison of the editing efficiency between Cas9 and Cas9-Act3.0 with both 20- and 15-nt protospacers. The Cas9-Act3.0 system here consists of a catalytically active Cas9 nuclease and MS2 bacteriophage coat protein (MCP)-SunTag-activator complex, and a gR1.0. Three biological replicates were performed for each target site. Representative gel images are shown. Each dot represents an individual biological replicate. Error bar represents the mean ± s.d. (n = 3 independent experiments). *P* values were obtained using the two-tailed Student's t-test. **c**, Cas9-Act3.0-induced gene activation with different protospacer length in gR2.0. The Cas9-Act3.0 system here consists of a catalytically active Cas9 nuclease and MS2 bacteriophage coat protein (MCP)-SunTag-activator complex, and a sgRNA2.0 (gR2.0) scaffold. T-DNA vectors without sgRNAs served as the negative control (CTRL). *OsTubulin* was selected as the endogenous control gene. Each dot represents an individual biological replicate. Error bar represents the mean ± s.d. (n = 3 independent experiments).

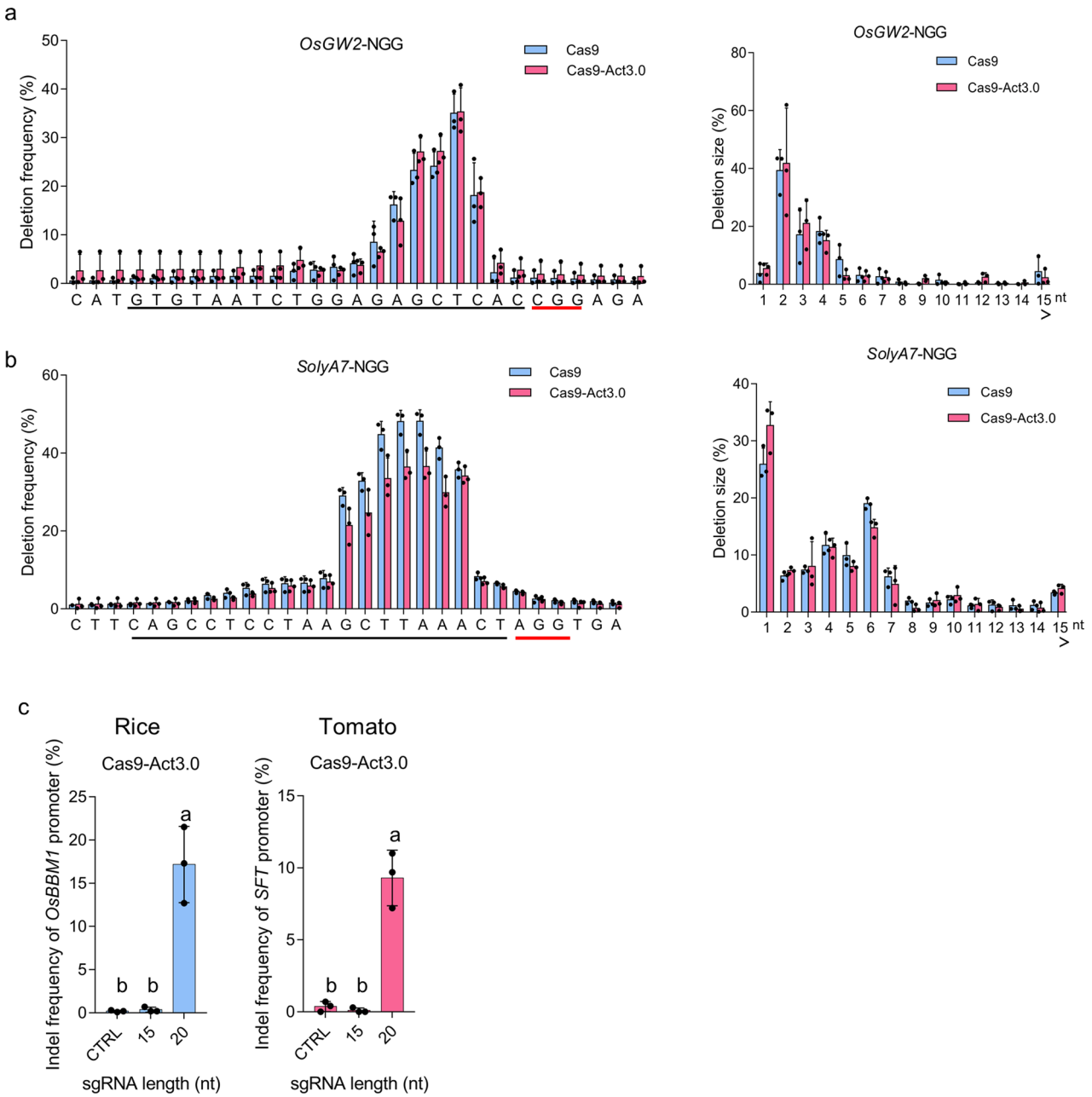

Extended Data Fig. 2 | Cleavage activity and deletion profiles of Cas9-Act3.0 in both rice and tomato protoplasts. a,b, Comparison of the deletion position and size between Cas9 and Cas9-Act3.0 in rice (**a**) and tomato (**b**) protoplasts based on NGS data. Frequencies of deletion position were calculated using the number of reads with deletions at designated nucleotide position divided by the total reads with deletions. PAM is highlighted in red underline and protospacer sequence is highlighted in black underline. Frequencies of deletion size were calculated using the number of reads with designated size deletion divided by the total reads with deletions. Each dot represents an individual biological replicate. Error bar represents the mean ± s.d. (n = 3 independent experiments). **c**, Cleavage activity of Cas9-Act3.0 with 15-nt and 20-nt protospacers at the *OsBBM1* and *SFT* promoters. One 15-nt and 20-nt protospacer for each of *OsBBM1* and *SFT* was separately cloned into the gR2.0 scaffold. One 20-nt protospacer for each of *OsGW2, OsGN1a,* and *SolyA7* was separately cloned into the gR1.0 scaffold. T-DNA vectors without sgRNAs served as the negative control (CTRL). Each dot represents an individual biological replicate. Error bar represents the mean ± s.d. (n = 3 independent experiments). The different letters indicate significantly different mean values at $P < 0.05$ (one-way analysis of variance (ANOVA) with post-hoc Tukey test).

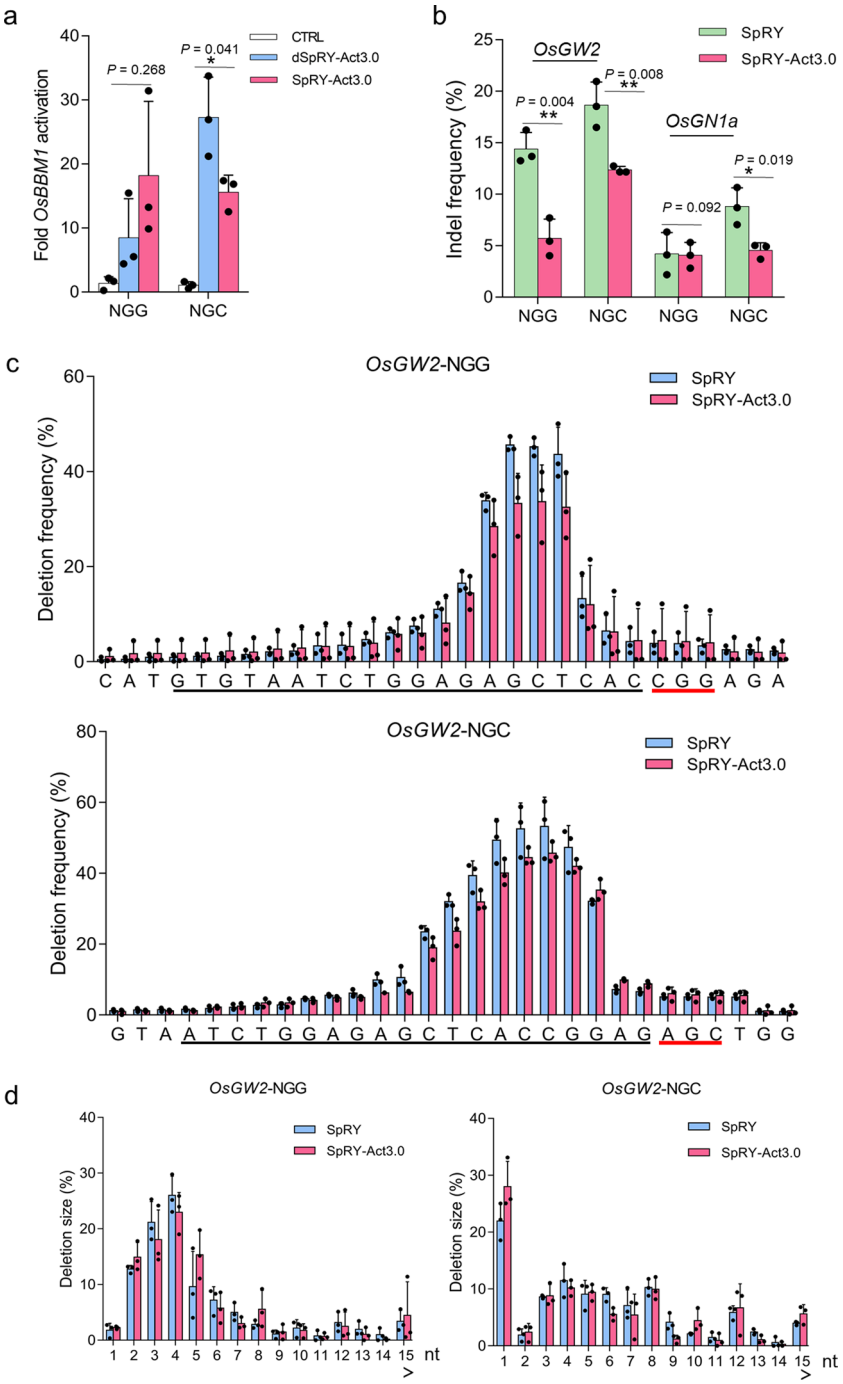

Extended Data Fig. 3 | Development and characterization of the PAM-less SpRY-Act3.0 system. a,b, Determination of SpRY-Act3.0-based-simultaneous gene activation **(a)** and targeted mutagenesis **(b)** in rice protoplasts at both NGG and NGC protospacer adjacent motifs (PAMs). One 15-nt protospacer of *OsBBM1* each at both NGG and NGC PAMs was separately cloned into gR2.0 for SpRY-Act3.0-mediated gene activation. One 20-nt protospacer each for *OsGW2* and *OsGN1a* at both NGG and NGC PAMs was separately cloned into gR1.0 for SpRY-Act3.0-mediated genome editing. The indel mutation assays were analysed by NGS. The dSpRY-Act3.0 activation system and SpRY nuclease were selected as references for comparing SpRY-Act3.0-mediated simultaneous gene activation and indel mutation, respectively. T-DNA vectors without sgRNAs served as the negative control (CTRL). *OsTubulin* was selected as the endogenous control gene. Each dot represents an individual biological replicate. Error bar represents the mean ± s.d. (n = 3 independent experiments). *P* values were obtained using the two-tailed Student's t-test. $^{*}P < 0.05$, $^{**}P < 0.01$. **c**, Deletion position analysis of both SpRY and SpRY-Act3.0 systems in rice protoplasts based on NGS data. Deletion frequencies were calculated using the number of reads with deletions at designated nucleotide position divided by the total reads with deletions. PAM is highlighted in red underline and protospacer sequence is highlighted in black underline. Each dot represents an individual biological replicate. Error bar represents the mean ± s.d. (n = 3 independent experiments). **d**, Deletion size analysis of both SpRY and SpRY-Act3.0 systems in rice protoplasts. Deletion frequencies were calculated using the number of reads with designated size deletion divided by the total reads with deletions. Each dot represents an individual biological replicate. Error bar represents the mean ± s.d. (n = 3 independent experiments).

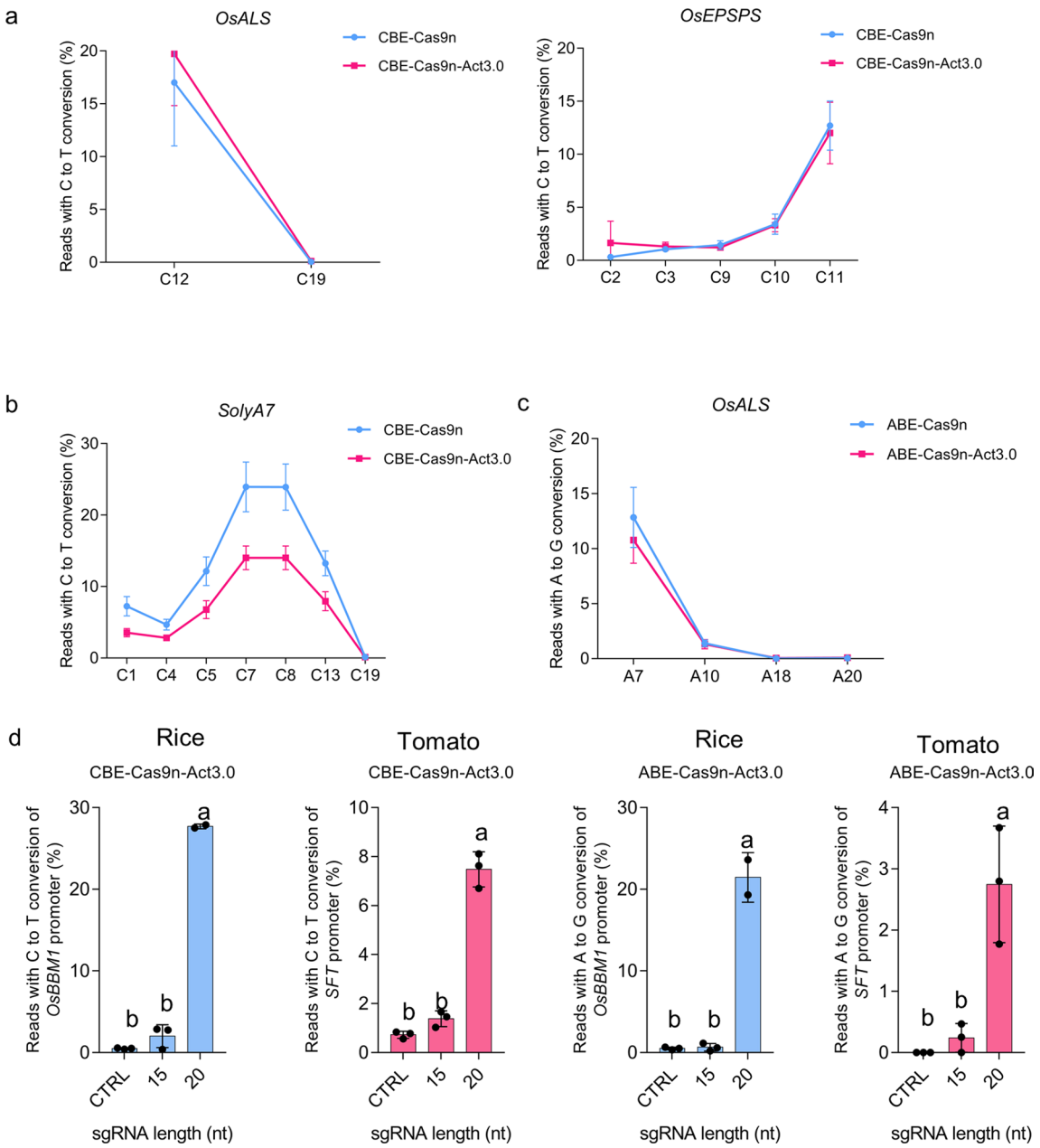

Extended Data Fig. 4 | Editing activity and window analysis of CBE-Cas9n-Act3.0 and ABE-Cas9n-Act3.0 systems in rice and tomato protoplasts. a,b, Editing window analysis of CBE-Cas9n and CBE-Cas9n-Act3.0 systems in rice **(a)** and tomato **(b)** protoplasts based on NGS data. The C to T conversion efficiencies were analysed by the CRISPR RGEN tools. 'Cn' indicates the position of target C in the protospacer. Error bar represents the mean ± s.d. (n = 3 independent experiments). **c**, Editing window analysis of ABE-Cas9n and ABE-Cas9n-Act3.0 base editors in rice protoplasts. The A to G conversion efficiencies were analysed by the CRISPR RGEN tools. 'An' indicates the position of target A in the protospacer. Error bar represents the mean ± s.d. (n = 3 independent experiments). **d**, Editing activity of CBE-Cas9n-Act3.0 and CBE-Cas9n-Act3.0 systems with 15-nt and 20-nt protospacers at the *OsBBM1* and *SFT* promoters. One 15-nt and 20-nt protospacer for each of *OsBBM1* and *SFT* was separately cloned into the gR2.0 scaffold. One 20-nt protospacer for each of *OsALS*, *OsEPSPS*, and *SolyA7* was separately cloned into the gR1.0 scaffold. T-DNA vectors without sgRNAs served as the negative control (CTRL). Each dot represents an individual biological replicate. Error bar represents the mean ± s.d. (n = 3 independent experiments). The different letters indicate significantly different mean values at $P < 0.05$ (one-way analysis of variance (ANOVA) with post-hoc Tukey test).

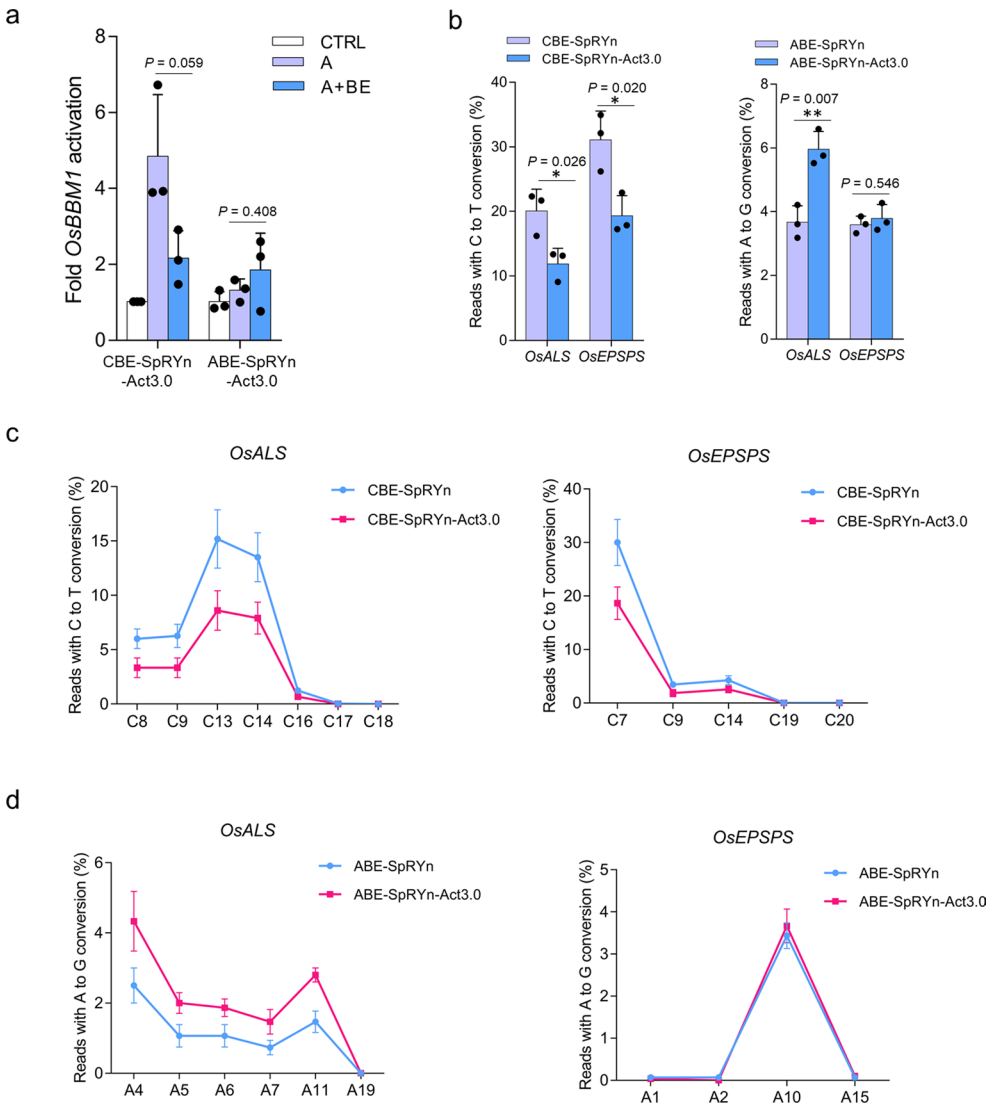

Extended Data Fig. 5 | Characterization of the CBE-SpRYn-Act3.0 and ABE-SpRYn-Act3.0 systems. a,b, Determination of CBE-SpRYn-Act3.0 and ABE-SpRYn-Act3.0-based-simultaneous gene activation **(a)** and base editing **(b)** efficiency in rice protoplasts. One 15-nt protospacer of *OsBBM1* was cloned into gR2.0 for CBE/ABE-SpRYn-Act3.0-mediated gene activation. One 20-nt protospacer for both *OsALS* and *OsEPSPS* each was separately cloned into gR1.0 for CBE/ABE-SpRYn-Act3.0-mediated base editing. A indicates CBE/ABE-SpRYn-Act3.0-mediated target gene activation with only gR2.0 scaffold. A + BE indicates CBE/ABE-SpRYn-Act3.0-mediated simultaneous gene activation and base editing with both gR1.0 and gR2.0 scaffolds. To compare base editing efficiency, CBE-SpRYn and ABE-SpRYn were selected as references in CBE-SpRYn-Act3.0 and ABE-SpRYn-Act3.0-mediated A + BE assays, respectively. T-DNA vectors without sgRNAs served as the negative control (CTRL). *OsTubulin* was selected as the endogenous control gene. Each dot represents an individual biological replicate. Error bar represents the mean ± s.d. (n = 3 independent experiments). *P* values were obtained using the two-tailed Student's t-test. $^{*}P < 0.05$, $^{**}P < 0.01$. **c,d**, Editing window analysis of CBE-SpRYn-Act3.0 **(c)** and ABE-SpRYn-Act3.0 **(d)** base editors in rice protoplasts. The C to T and A to G conversion efficiencies were analysed by the CRISPR RGEN tools. 'Cn' and 'An' indicate the position of target C and A in the protospacer, respectively. Error bar represents the mean ± s.d. (n = 3 independent experiments).

a

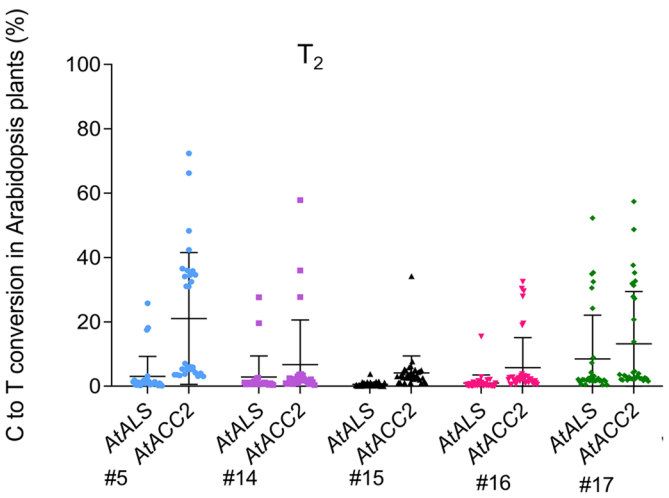

b

atalsatacc2

#17-11

	AtALS	Gln			Val			Pro to Ser			Arg to Cys			Arg to Cys			Met			Ile				
		C	A	A	G	T	**C**	**C**	**C**	T	**C**	G	T	**C**	G	T	A	T	G	A	T	**T**	**G**	**G**
#17-11	T	0	0	0	0	100	29	30	0.1	100	30	0	100	30	0	100	0	100	0	0	100	100	0	0
	C	100	0	0	0	0	71	71	100	0	70	0	0	70	0	0.1	0	0.1	0	0	0	0.1	0	0
	AtACC2	Asp			Gln			Pro to Leu			Ile			Ile			Leu			Thr				
		G	A	**C**	**C**	A	A	**C**	**C**	G	A	T	**C**	A	T	**C**	T	T	G	A	**C**	**C**	**G**	**G**
	T	0	0	0	0.1	0	0	33	31	0	0	100	35	0	100	0.1	100	100	0	0	0.1	0.2	0	0
	C	0	0	100	100	0	0	66	69	0	0	0	65	0	0	100	0	0	0	0	100	100	0	0

#14-23

	AtALS	Gln			Val			Pro to Ser			Arg to Cys			Arg to Cys			Met			Ile				
		C	A	A	G	T	**C**	**C**	**C**	T	**C**	G	T	**C**	G	T	A	T	G	A	T	**T**	**G**	**G**
#14-23	T	0	0	0	0	100	5.8	10	7.7	100	19	0	100	8.5	0	100	0	100	0	0	100	100	0	0
	C	100	0	0	0	0	94	90	92	0.1	81	0	0	91	0	0.1	0	0	0	0	0	0	0	0
	AtACC2	Asp			Gln			Pro to Leu			Ile			Ile			Leu			Thr				
		G	A	**C**	**C**	A	A	**C**	**C**	G	A	T	**C**	A	T	**C**	T	T	G	A	**C**	**C**	**G**	**G**
	T	0	0	0.1	1.4	0	0	7.1	27	0	0	100	40	0	100	0.4	100	100	0	0	0.1	0.1	0	0
	C	0	0	100	99	0	0	91	73	0	0	0	59	0	0	100	0	0.1	0	0	100	100	0	0

atalsAtACC2

	AtALS	Gln			Val			Pro to Ser			Arg to Cys			Arg to Cys			Met			Ile				
		C	A	A	G	T	**C**	**C**	**C**	T	**C**	G	T	**C**	G	T	A	T	G	A	T	**T**	**G**	**G**
#5-6	T	0	0	0	0	100	0.2	0.5	0.3	100	26	0	100	0.4	0	100	0	100	0	0	100	100	0	0
	C	100	0	0	0	0	100	100	100	0	74	0	0	100	0	0	0	0	0	0	0	0.2	0	0
#14-5	T	0	0	0	0	100	0.1	0.1	0.1	100	28	0	100	27	0	100	0	100	0	0	100	100	0	0
	C	100	0	0	0	0.1	100	73	100	0	72	0	0	73	0	0	0	0	0	0	0	0	0	0
#17-7	T	0	0	0	0	100	0.8	0.9	0.2	100	35	0	100	35	0	100	0	100	0	0	100	100	0	0
	C	100	0	0	0	0.1	99	99	100	0.1	65	0	0	65	0	0.1	0	0	0	0	0	0.1	0	0

AtALSatacc2

	AtACC2	Asp			Gln			Pro to Leu			Ile			Ile			Leu			Thr				
		G	A	**C**	**C**	A	A	**C**	**C**	G	A	T	**C**	A	T	**C**	T	T	G	A	**C**	**C**	**G**	**G**
#5-22	T	0	0	0.1	0	0	0	1	37	0	0	100	72	0	100	0	100	100	0	0	0.1	0.3	0	0
	C	0	0	100	100	0	0	63	63	0	0	0	26	0	0	100	0	0	0	0	100	100	0	0
#5-26	T	0.1	0	0.1	0	0	0	1	0.6	0	0	100	66	0	100	0	100	100	0	0	0.2	0.2	0	0
	C	0	0	100	100	0	0	99	99	0	0	0	34	0	0	100	0.1	0	0	0	100	100	0	0
#15-4	T	0	0	0	0	0	0	28	30	0	0	100	34	0	100	0	100	100	0	0	0	0.1	0	0
	C	0	0	100	100	0	0	70	70	0	0	0	64	0	0	100	0.2	0	0	0	100	100	0	0

Extended Data Fig. 6 | Mutation and genotype analysis of CBE-Cas9n-Act3.0-mediated T2 standard flowering plants (transgene-free). a, Mutation analysis of T_2 T-DNA free standard flowering populations for the CBE-Cas9n-Act3.0 system. The base editing frequencies of examined transgene-free plants were determined by NGS. Each dot indicates an individual plant. Error bar represents the mean ± s.d. (n = 29, 24, 37, 38 and 32 independent plants for #5, #14, #15, #16 and #17, respectively). **b**, Representative genotypes of *atalsatacc2*, *atalsAtACC2* and *AtALSatacc2* plants in T_2 T-DNA free standard flowering populations. Three kinds of genotypes (*atalsatacc2*, *atalsAtACC2*, and *AtALSatacc2*) are identified in CBE-Cas9n-Act3.0-mediated standard flowering (transgene-free) populations. The PAM is highlighted in yellow. The DNA bases C in the protospacer sequence are highlighted in red, and the other DNA bases of the protospacer are highlighted in green. The symbols above the protospacer sequence indicate amino acids. The numbers below the protospacer sequence indicate the percentage of DNA base T or C in total reads. The base editing efficiencies were analysed by the CRISPR RGEN tools.

a

Cas9-Act3.0		*AtFT*	1	2	3	4	5	6	7	8	9	10	11	12	13	14	15
Extra-early flowering plants	T_2-#2	sgRNA1	n/a	n/a	n/a	n/a	n/a	n/a	n/a	n/a	n/a	n/a	n/a	n/a	n/a	n/a	n/a
		sgRNA2	n/a	n/a	n/a	n/a	n/a	n/a	n/a	n/a	n/a	n/a	n/a	n/a	n/a	n/a	n/a
	T_2-#4	sgRNA1	n/a	n/a	n/a	n/a	n/a	n/a	n/a	n/a	n/a	n/a	n/a	n/a	n/a	n/a	n/a
		sgRNA2	n/a	n/a	n/a	n/a	n/a	n/a	n/a	n/a	n/a	n/a	n/a	n/a	n/a	n/a	n/a
	T_2-#11	sgRNA1	n/a	n/a	n/a	n/a	n/a	n/a	n/a	n/a	n/a	n/a	n/a	n/a	n/a	n/a	n/a
		sgRNA2	n/a	n/a	n/a	n/a	n/a	n/a	n/a	n/a	n/a	n/a	n/a	n/a	n/a	n/a	n/a
Standard flowering plants (T-DNA free)	T_2-#1	sgRNA1	n/a	n/a	n/a	n/a	n/a	n/a	n/a	n/a	n/a	n/a	n/a	n/a	n/a	n/a	n/a
			n/a	n/a	n/a	n/a	n/a	n/a	n/a	n/a							
		sgRNA2	n/a	n/a	n/a	1d1/1,527	n/a	n/a	n/a	n/a	n/a	n/a	n/a	n/a	n/a	n/a	n/a
			n/a	n/a	n/a	n/a	n/a	n/a	n/a	n/a							
	T_2-#2	sgRNA1	n/a	n/a	n/a	n/a	n/a	n/a	n/a	n/a	n/a	n/a	1d1/838	n/a	n/a	n/a	n/a
			n/a	n/a	n/a	n/a	n/a	n/a	n/a	n/a							
		sgRNA2	n/a	n/a	n/a	n/a	n/a	n/a	n/a	n/a	n/a	n/a	n/a	n/a	n/a	n/a	n/a
			n/a	n/a	n/a	n/a	n/a	n/a	n/a	n/a							

b

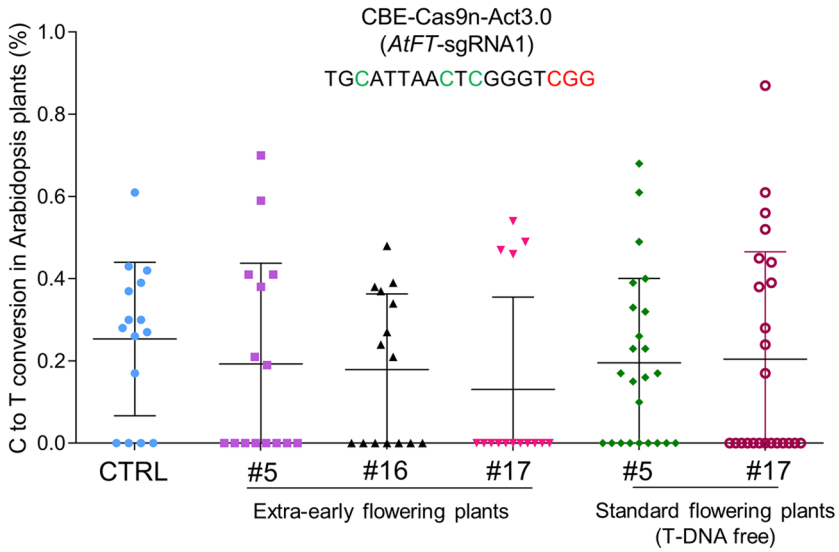

Extended Data Fig. 7 | Undetectable off-target genome-editing activity by Cas9-Act3.0 and CBE-Cas9n-Act3.0 at the *AtFT* promoter with 15-nt protospacers. a, Identification of Cas9-Act3.0-mediated potential indel mutations at two *AtFT* target sites in both T_2 extra-early flowering and T-DNA free standard flowering plants. Three and two independent lines were selected for extra-early flowering and T-DNA free standard flowering groups, respectively. Approximately 15 to 23 individual plants were examined for each line. n/a, no indel mutation was detected. 1d1/1,527, one 1-bp deletion event detected in a total of 1,527 reads. 1d1/838, one 1-bp deletion event was detected in a total of 838 reads. The indel mutations were analysed by CRISPResso2. **b**, Identification of CBE-Cas9n-Act3.0-mediated potential base editing at *AtFT*-sgRNA1 target site in both T_2 extra-early flowering and T-DNA free standard flowering plants. Three and two independent lines were selected for extra-early flowering and T-DNA free standard flowering groups, respectively. CTRL represents wild-type plants. Approximately 15 to 24 individual plants were examined for each line. The PAM of *AtFT*-sgRNA1 is highlighted in red and DNA bases C in the protospacer sequence are highlighted in green. The base editing efficiencies were analysed by the CRISPR RGEN tools. Each dot represents an individual plant. Error bar represents the mean ± s.d. (n = 15 independent plants for CTRL, #5, #16 and #17, n = 24 independent plants for T-DNA free lines #5 and #17). Note the *AtFT*-sgRNA2 doesn't contain any DNA base C and hence was not analysed for C to T base editing.

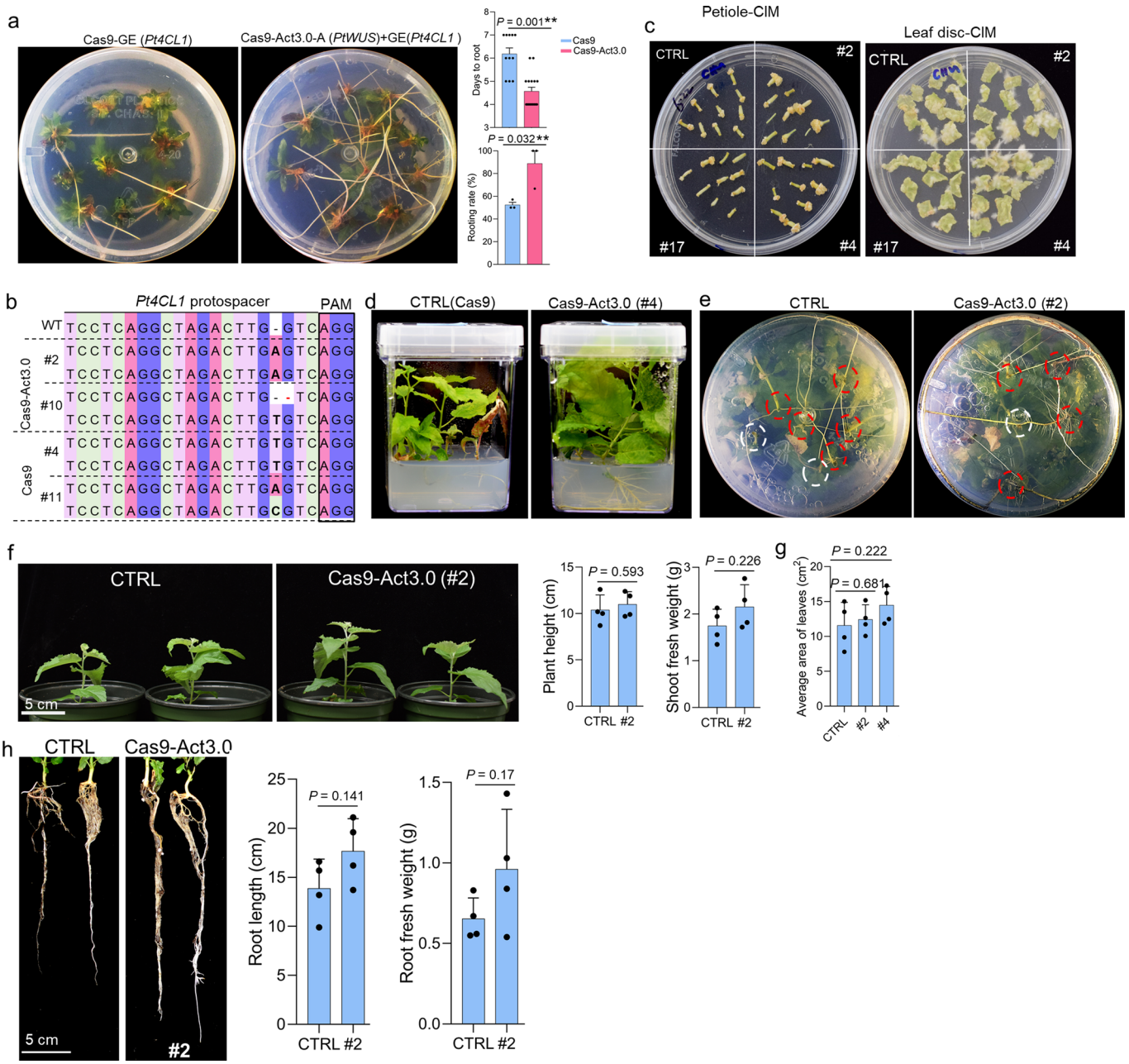

Extended Data Fig. 8 | Cas9-Act3.0 promotes *de novo* callus and root organogenesis from petiole and stem cuttings by activation of *PtWUS* in poplar. **a**, Cas9-Act3.0 promotes root initiation by activation of *PtWUS* in poplar. Two gR2.0 with 15-nt protospacers and one gR1.0 with 20-nt protospacer were used for *PtWUS* and *Pt4CL1*, respectively. All transgenic plants were grown in the root-induction medium (RIM) with hygromycin selection. For days to root, error bar represents the mean ± s.d. (n = 11 and 13 independent plants for Cas9 and Cas9-Act3.0, respectively). For rooting rate, error bar represents the mean ± s.d. (n = 3 biological replicates). The root initiation rate was evaluated on the 7th day after transgenic shoots were transferred to RIM. **b**, Representative genotypes of Cas9-Act3.0 and Cas9-mediated T0 *Pt4CL1* mutants. The red dash indicates a nucleotide deletion. The bold DNA bases indicate insertion. PAM, protospacer adjacent motif. **c**, Cas9-Act3.0 promotes *de novo* callus formation from petiole cuttings and leaf-disc regeneration by activation of *PtWUS*. Petiole cuttings and leaf discs from CTRL and *PtWUS*-activation poplar plants were cultured on callus induction medium (CIM) for two weeks. Representative *PtWUS*-activation lines including #2, #4, and #17 are shown. **d**, The Cas9-Act3.0 promotes shoot growth of stem cuttings by activation of *PtWUS* in poplar. Four stem cuttings from each of CTRL and *PtWUS*-activation line (#4) were cultured in one magenta box with root-induction medium (RIM). **e**, Cas9-Act3.0 promotes *de novo* root initiation of stem cuttings by activation of *PtWUS* in poplar. Five to seven stem cuttings were cultured in one magenta box with the root-induction medium. Red dash cycles indicate successful root initiation and white dash cycles indicate failed root initiation. **f,h**, Representative shoot (**f**) and root (**h**) phenotype of CTRL and *PtWUS*-activation poplar line (#2). Plants were grown in soil under the same cultivation conditions for six weeks. Error bar represents the mean ± s.d. (n = 4 independent plants). **g**, Leaf area analysis of CTRL and *PtWUS*-activation poplar lines (#2 and #4). Error bar represents the mean ± s.d. (n = 4 independent plants). *P* values in **a, f-h** were obtained using the two-tailed Student's t-test. $^{**}P < 0.01$.

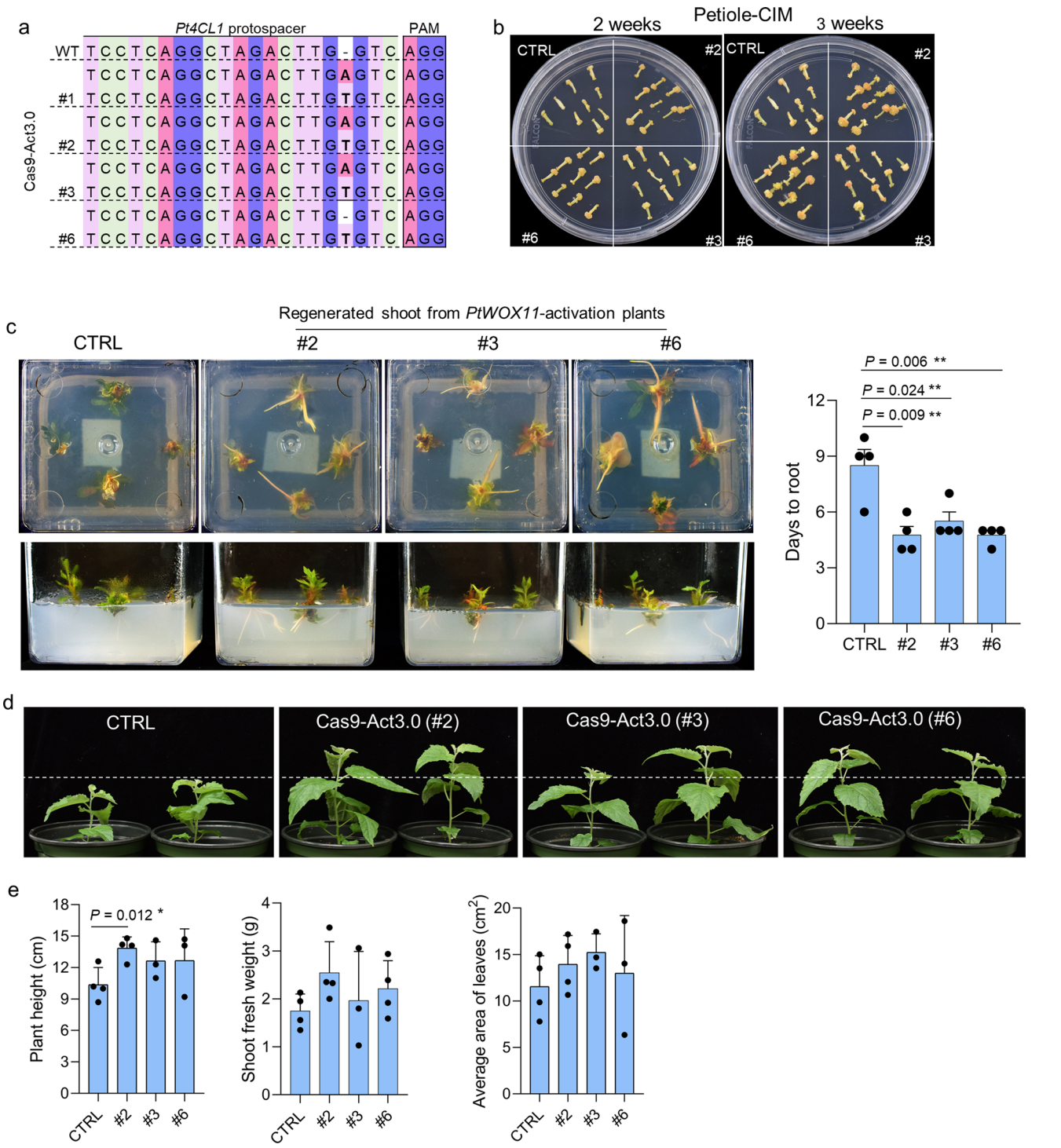

Extended Data Fig. 9 | Cas9-Act3.0 promotes *de novo* callus and root organogenesis of petiole and shoot regenerated from *PtWOX11*-activation poplar. a, Representative genotypes of Cas9-Act3.0 and Cas9-mediated T_0 *Pt4CL1* mutants. The four DNA bases A, T, C, G are marked in different colours. The red dash indicates a nucleotide deletion. The bold DNA bases indicate insertion. PAM, protospacer adjacent motif. b, Cas9-Act3.0 promotes de novo callus formation from petiole cuttings by activation of *PtWOX11*. Petiole cuttings from CTRL and *PtWOX11*-acitvation plants were cultured on callus induction medium (CIM) for three weeks. Representative petioles of *PtWOX11*-acitvation lines including #2, #3, and #6 are shown. **c**, The Cas9-Act3.0 system promotes root initiation of shoots regenerated from the *PtWOX11*-activation poplar. Four regenerated shoots from each of CTRL and *PtWOX11*-acitvation plants were cultured in one magenta box with root-induction medium (RIM) for seven days. Representative root and shoot of CTRL and *PtWOX11*-acitvation lines are shown. Error bar represents the mean ± s.d. (n = 4 independent plants). **d**, Representative shoots of CTRL and *PtWOX11*-acitvation lines. Plants were grown in soil under the same cultivation conditions for six weeks. Three or four independent plants were examined for both CTRL and *PtWOX11*-acitvation lines. e, Leaf area analysis of CTRL and *PtWOX11*-activation poplar lines. Each dot indicates the average area of all leaves for an individual plant. Error bar represents the mean ± s.d. (n = 4 independent plants). *P* values in **c,e** were obtained using the two-tailed Student's t-test. $^*P < 0.05$, $^{**}P < 0.01$.

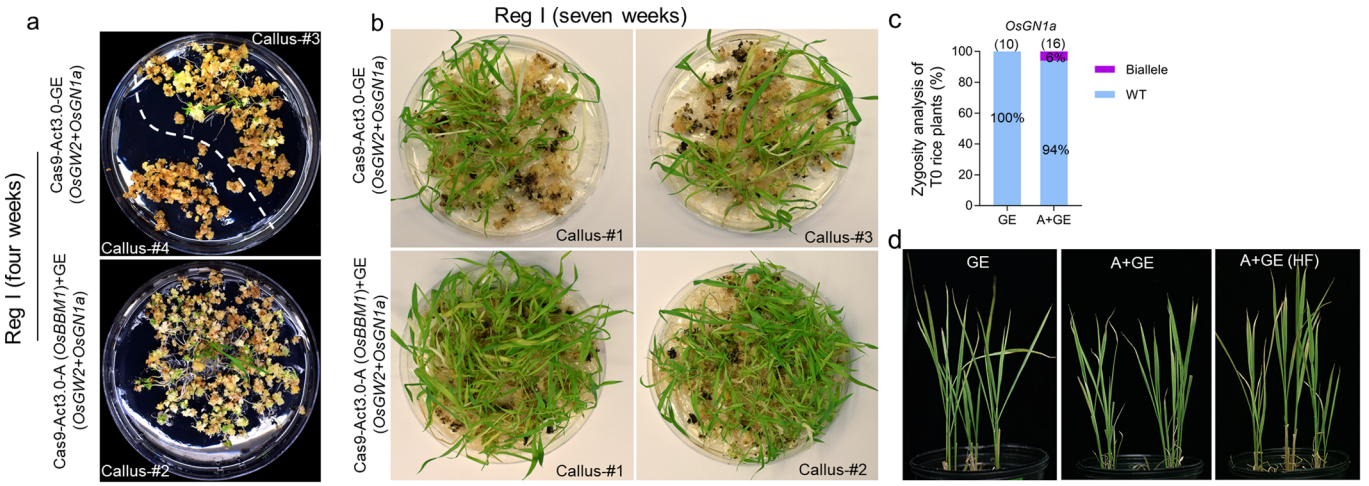

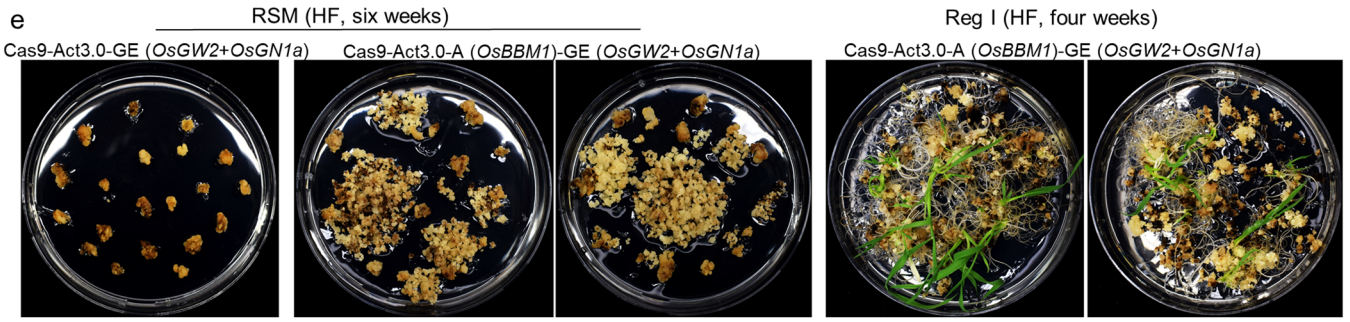

f

Callus	Cas9-Act3.0	
	GE	A+GE (HF)
Agro-infection	75	77
Hyg-resistance	2 (2.6%)	24 (31.6%)
Regeneration (two weeks)	0	10 (41.7%)
Regeneration (four weeks)	1	15 (62.5%)

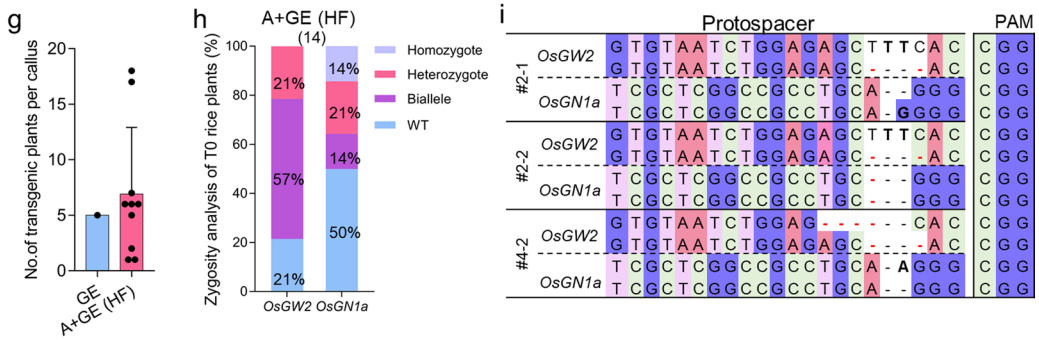

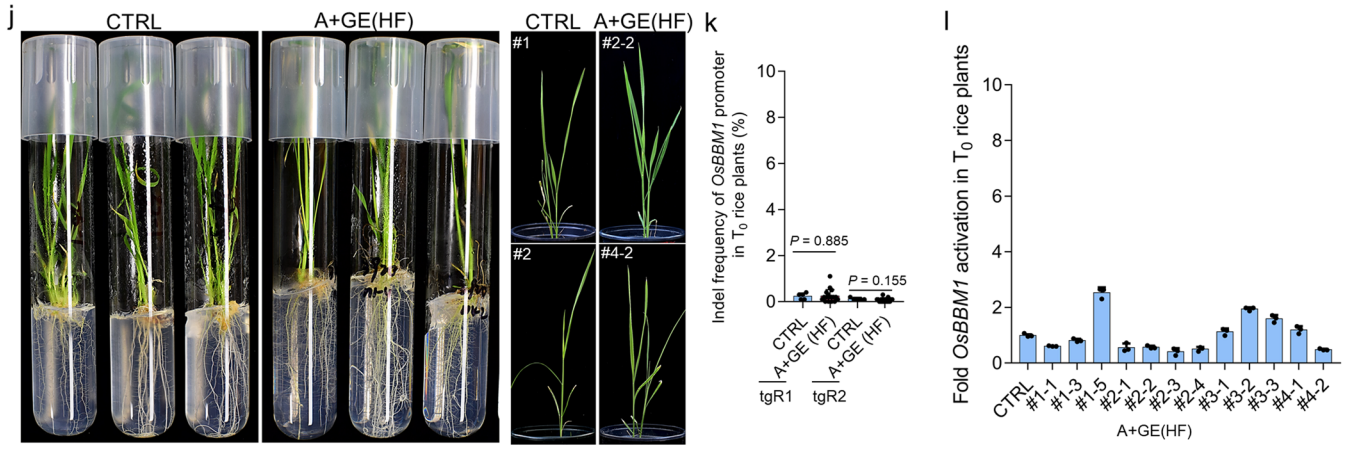

Extended Data Fig. 10 | See next page for caption.

Extended Data Fig. 10 | Cas9-Act3.0 promotes callus regeneration and enriches heritable targeted mutations by activation of *OsBBM1* in rice. **a,b**, Representative images of Cas9-Act3.0-induced shoot regeneration by activation of *OsBBM1* at four **(a)** and seven **(b)** weeks. The calli of both vectors were grown on regeneration I (Reg I) medium for seven weeks by subculturing every two weeks. **c**, Zygosity analysis of Cas9-Act3.0-mediated T_0 lines at the *OsGN1a* target site. A total of 10 and 16 individual transgenic plants were examined for Cas9-Act3.0-based GE and A+GE vectors, respectively. GE, genome editing. A+GE, simultaneous gene activation and editing. **d,j**, Representative images of Cas9-Act3.0-induced rice plants from hormone-containing and hormone-free (HF) mediums. **e**, Representative images of Cas9-Act3.0-mediated callus induction and regeneration by activating *OsBMM1* in a HF manner. RSM, rice selection medium. All calli were subcultured with HF fresh medium every two weeks. **f**, Efficiency of Cas9-Act3.0-callus induction and regeneration in a HF manner. All calli were cultured under the same conditions. **g**, Number of regenerated transgenic plants per Cas9-Act3.0-mediated callus in a HF manner. Each dot indicates the seedling number generated from one transgenic callus. Error bar represents the mean ± s.d. (n = 10 independent calli). **h**, Zygosity analysis of Cas9-Act3.0-mediated T_0 *OsGW2OsGN1a* mutants in a HF manner. The frequencies of each zygotic type are shown as percentages. A total of 14 individual transgenic plants were examined using NGS. **i**, Representative genotypes of Cas9-Act3.0-mediated T_0 *OsGW2OsGN1a* mutants in a HF manner. The red dash indicates a nucleotide deletion. The black dash indicates a blank space. The bold DNA bases indicate insertion. PAM, protospacer adjacent motif. **k**, Analysis of the cleavage activity of Cas9-Act3.0 at the target sites of *OsBBM1* promoter in rice plants. Both tgR1 and tgR2 of a 15-nt protospacer were used for OsBBM1 activation. Error bar represents the mean ± s.d. (n = 5 and 18 independent plants for CTRL and A+GE, respectively). *P* values were obtained using the two-tailed Student's t-test. **l**, Determination of *OsBBM1* activation level in Cas9-Act3.0-mediated HF edited plants using qRT-PCR. Leaf tissue was sampled for total RNA extraction. CTRL represents the mixed sample from three individual plants. Error bar represents the mean ± s.d. (n = 3 technical replicates).

nature research

Corresponding author(s): Yiping Qi

Last updated by author(s): 04/06/2022

Reporting Summary

Nature Research wishes to improve the reproducibility of the work that we publish. This form provides structure for consistency and transparency in reporting. For further information on Nature Research policies, see Authors & Referees and the Editorial Policy Checklist.

Statistics

For all statistical analyses, confirm that the following items are present in the figure legend, table legend, main text, or Methods section.

n/a	Confirmed	
☐	☒	The exact sample size (*n*) for each experimental group/condition, given as a discrete number and unit of measurement
☐	☒	A statement on whether measurements were taken from distinct samples or whether the same sample was measured repeatedly
☐	☒	The statistical test(s) used AND whether they are one- or two-sided *Only common tests should be described solely by name; describe more complex techniques in the Methods section.*
☒	☐	A description of all covariates tested
☒	☐	A description of any assumptions or corrections, such as tests of normality and adjustment for multiple comparisons
☐	☒	A full description of the statistical parameters including central tendency (e.g. means) or other basic estimates (e.g. regression coefficient) AND variation (e.g. standard deviation) or associated estimates of uncertainty (e.g. confidence intervals)
☐	☒	For null hypothesis testing, the test statistic (e.g. *F*, *t*, *r*) with confidence intervals, effect sizes, degrees of freedom and *P* value noted *Give P values as exact values whenever suitable.*
☒	☐	For Bayesian analysis, information on the choice of priors and Markov chain Monte Carlo settings
☒	☐	For hierarchical and complex designs, identification of the appropriate level for tests and full reporting of outcomes
☒	☐	Estimates of effect sizes (e.g. Cohen's *d*, Pearson's *r*), indicating how they were calculated

Our web collection on statistics for biologists contains articles on many of the points above.

Software and code

Policy information about availability of computer code

Data collection	None used
Data analysis	SnapGene 4.3.11 was used to analyze and construct DNA vectors. BioRad CFX Manager (Version 3.1) and Excel 2021 were used to analyze qRT-PCR data. Promoter sequences were obtained from Phytozome v13 database (https://phytozome.jgi.doe.gov/pz/portal.html). Biorender was used to draw the cartoons displayed in this work.

For manuscripts utilizing custom algorithms or software that are central to the research but not yet described in published literature, software must be made available to editors/reviewers. We strongly encourage code deposition in a community repository (e.g. GitHub). See the Nature Research guidelines for submitting code & software for further information.

Data

Policy information about availability of data

All manuscripts must include a data availability statement. This statement should provide the following information, where applicable:

- Accession codes, unique identifiers, or web links for publicly available datasets
- A list of figures that have associated raw data
- A description of any restrictions on data availability

All generated and processed data from this study are included in the published article and its Supplementary Information. The Golden Gate and Gateway compatible vectors for the CRISPR–Combo systems were deposited to Addgene: pYPQ-Cas9-Act3.0 (no.178954), pYPQ-CBE-Cas9n-Act3.0 (no.178955), pYPQ-ABE-Cas9n-Act3.0 (no.178956), pYPQ-SpRY-Act3.0 (no.178957), pYPQ-CBE-SpRYn-Act3.0 (no.178958), pYPQ-ABE-SpRYn-Act3.0 (no.178959), pYPQ132-tRNA (no.179211), pYPQ133-tRNA (no.179212), pYPQ134-tRNA (no.179213), pYPQ134B (no.179216). The sequence data of targeted genes can be found from The Arabidopsis Information Resource (https://www.Arabidopsis.org/), Rice Genome Annotation Project (http://rice.uga.edu/) Solanaceae Genomics Network (https://solgenomics.net/) or Phytozome (https://phytozome-next.jgi.doe.gov/) using their locus identifiers as follows: OsBBM1 (LOC_Os11g19060), OsGW2 (LOC_Os02g14720), OsGN1a (LOC_Os01g10110), OsALS (LOC_Os02g30630), OsEPSPS (LOC_Os06g04280), OsYSA (LOC_Os03g40020), OsMAPK5 (LOC_Os03g17700), AtFT (AT1G65480), AtAP1 (AT1G69120), AtPYL1 (AT5G46790), AtALS (AT3G48560), AtACC2 (AT1G36180), PtWUS (Potri.005G114700),

PtWOX11 (Potri.013G066900), PtARK1 (Potri.011G011100), Pt4CL1 (Potri.001G036900), SFT (Solyc03g063100), SolyA7 (Solyc01g010970). The NGS data have been deposited to National Center for Biotechnology Information (accession code PRJNA779678).

Field-specific reporting

Please select the one below that is the best fit for your research. If you are not sure, read the appropriate sections before making your selection.

☒ Life sciences ☐ Behavioural & social sciences ☐ Ecological, evolutionary & environmental sciences

For a reference copy of the document with all sections, see nature.com/documents/nr-reporting-summary-flat.pdf

Life sciences study design

All studies must disclose on these points even when the disclosure is negative.

Sample size	About 100,000 cells are sufficient for RNA extraction using TRIzol method. For rice and tomato protoplast assays, 360 µL rice protoplasts (2x1,000,000 cells/mL) or tomato protoplasts (1x1,000,000 cells/mL) were used for PEG-mediated transfection per sample. The cell counting was performed using the disposable hemocytometer DHC-N01 with a microscope. For stable transformation, around 150 individual transgenic plants were evaluated in T1 Arabidopsis plants. A total of 1,500 and 300 individual transgenic plants were evaluated in T2 and T3 Arabidopsis plants, respectively. In poplar, around 50 individual transgenic plants were evaluated in T0 generation. In addition, around 150 petiole and 60 stem cuttings were examined. In rice, a total of 350 individual transgenic plants were evaluated in T0 generation. For statistical analysis, two-tailed Student's t-test and One-way ANOVA with Tukey test were used.
Data exclusions	No data was excluded.
Replication	For protoplast assays, three biological replicates were performed. For stable transformation, one or two biological replicates were performed for each experiment. For in-vitro regeneration, at least two biological replicates were analyzed. All data has been provided in the manuscript.
Randomization	For phenotypic characterization in all experiments, all seedlings were grown on the petri-dishes or in the pots. Plants were randomly placed across all samples and replicates.
Blinding	Blinding was not relevant to this study during data collection and analysis. Becasue the information for each protoplast sample or plant had been prelabelled before data collection and analysis.

Reporting for specific materials, systems and methods

We require information from authors about some types of materials, experimental systems and methods used in many studies. Here, indicate whether each material, system or method listed is relevant to your study. If you are not sure if a list item applies to your research, read the appropriate section before selecting a response.

Materials & experimental systems

n/a	Involved in the study
☒	☐ Antibodies
☒	☐ Eukaryotic cell lines
☒	☐ Palaeontology
☒	☐ Animals and other organisms
☒	☐ Human research participants
☒	☐ Clinical data

Methods

n/a	Involved in the study
☒	☐ ChIP-seq
☒	☐ Flow cytometry
☒	☐ MRI-based neuroimaging